INFRARED SPECTROMETER
CALIBRATION MONOCHROMATOR STUDY

Contract 950974
(Subcontract under NASA Contract NAS 7-100)

FINAL REPORT

Beckman

Prepared for
California Institute of Technology
Jet Propulsion Laboratory

Beckman Instruments, Inc., Space Engineering Department, Fullerton, California

54-730

Beckman®

INFRARED SPECTROMETER

CALIBRATION MONOCHROMATOR STUDY

FINAL REPORT

This work was performed for the Jet Propulsion Laboratory, California Institute of Technology, sponsored by the National Aeronautics and Space Administration under Contract NAS7-100.

Prepared by

B. D. Henderson
J. Zerucha

For

California Institute of Technology
Jet Propulsion Laboratory

Contract 950974
(Subcontract under NASA Contract NAS 7-100)

Beckman® INSTRUMENTS, INC.
SCIENTIFIC AND PROCESS
INSTRUMENTS DIVISION
FULLERTON, CALIFORNIA

FOREWORD

This Final Report on the Infrared Spectrometer Calibration Study conducted by Beckman Instruments, Inc. for the California Institute of Technology, Jet Propulsion Laboratory, describes the optical system which Beckman recommends for this instrument, and discusses the requirements for the various optical components to be utilized. The work on this project was performed under Contract 950974, which is a subcontract under NASA Contract NAS 7-100. The scope of the work is defined in the SCHEDULE included in the subject contract, which is reproduced on the following page.

Contract No. 950974

SCHEDULE

ARTICLE 1. STATEMENT OF WORK

(a) The Contractor shall:

(1) Conduct a study of the design of an Infrared Spectrometer Calibration Monochromator and provide a design specification for the optimum optical arrangement in accordance with the Beckman Technical Proposal CS 64-654, dated 25 June 1964,

(i) Aperture - f/3 or faster.

(ii) Slit:

(A) Height - 15mm minimum

(B) Width - variable 5 microns to 4mm

(C) Shape:

(I) Exit straight

(II) Entrance may be curved

(iii) Resolution at .3mm slit width shall equal 1000 (no overlapping orders).

(iv) Wavelength region 1μ to 15μ.

(v) Dimensions maximum 18" by 18" by 24".

(vi) Environmental operation shall be remotely adjustable for operation in vacuum of 10^{-6} Hg at temperature of 80°K.

(vii) Distribution of energy at the exit slit shall be determinable, assuming uniform illumination of the entrance slit.

(2) Provide one (1) vellum and ten (10) print copies of a Final Report which shall include, but not necessarily be limited to, the following:

(i) Outline of optical layout.

(ii) Optical components list specifying sizes, shapes, locations and tolerances and adjustments thereof.

(iii) Grating and/or prism or prisms specifications including the following details:

(A) Blaze

(B) Blaze Angle

(C) Spacing

(D) Energy Distribution

(iv) Filters, baffles and auxiliary device specifications.

(v) Summary of the work performed and any unique problems encountered and solutions or attempted solutions thereto.

TABLE OF CONTENTS

LIST OF ILLUSTRATIONS

LIST OF TABLES

INFRARED SPECTROMETER
CALIBRATION MONOCHROMATOR STUDY

FINAL REPORT

1. INTRODUCTION

The purpose of this study was to determine the optimal design for a calibration monochromator to be used to measure the quantitative performance of various spectrometers for use in space applications. The entrance optics of the calibration monochromator will be provided with a source or sources of radiation, and the monochromatic radiation passing through the exit slit is to have an accurately known spectral energy distribution. This output energy will be fed into the entrance slit of the monochromator under test by means of coupling optics. In order to insure satisfactory operation of the system, it is necessary that the slits and the dispersive element of the calibration monochromator be filled with absolutely uniform radiation. The coupling optics must similarly illuminate the monochromator under test with absolutely uniform illumination at both the entrance slit and the dispersive element of this monochromator.

Some optical coupling difficulties between the calibration monochromator and the monochromator under test may result from the optical configuration of the latter. The multi-detector monochromator which was designed for the Jet Propulsion Laboratory by Beckman Instruments, Inc. under contract #950880 is an example of this. This particular monochromator has its entrance slit

tilted from the vertical both forward and sidewise in order to assure optimal image orientation at the spectral image plane where the spectral images of the entrance slit must be properly oriented for reception by a multi-detector array. This monochromator also uses an entrance telescope consisting of a single off-axis spherical mirror. The combination of tilted slits and the off-axis telescope mirror creates difficult optical coupling problems, and coupling problems as serious as this may be anticipated for the calibration monochromator. The calibration monochromator design which has been developed in this study will provide high quality measurements of the performance of this multi-detector monochromator and its integral entrance telescope, and will be readily adaptable for use with other systems as well.

In the technical discussion to follow, the design of the calibration monochromator is presented, and methods of optically coupling the calibration monochromator to the multi-detector monochromator, and its entrance optics previously mentioned, are discussed. The techniques for designing coupling optics as developed here will be directly applicable to monochromators of other optical configurations.

2.0 TECHNICAL DISCUSSION

In order to uniformly fill with illumination the entrance slit and dispersive element or elements of the monochromator under test, a calibration monochromator must possess both greater slit height and slit width and greater numerical aperture than the test monochromator. The larger slit width requirements for the calibration monochromator means that this monochromator must gain additional dispersion by increase in focal length or by being a double monochromator.

2.1 The Calibration Monochromator

The calibration monochromator design developed as a result of this study has an 8 inch square dispersive aperture, and a square aperture f/number of f/2.5 (the ratio of the monochromator focal length to the average of the height and width of the aperture). This is equivalent, in optical efficiency, to f/2.1 for a circular aperture. This monochromator uses a single grating as the dispersive element and has a 20 inch (500 mm) focal length. The geometrical layout of the calibration monochromator presented in Figure 1 completely defines the monochromator.

2.1.1 Reasons for Choice of Monochromator Optics

Figure 1 shows that the monochromator optics which have been chosen make use of a single paraboloid collimating mirror with the entrance and exit slits in a common plane, and each slit is mounted as near the focal point of the

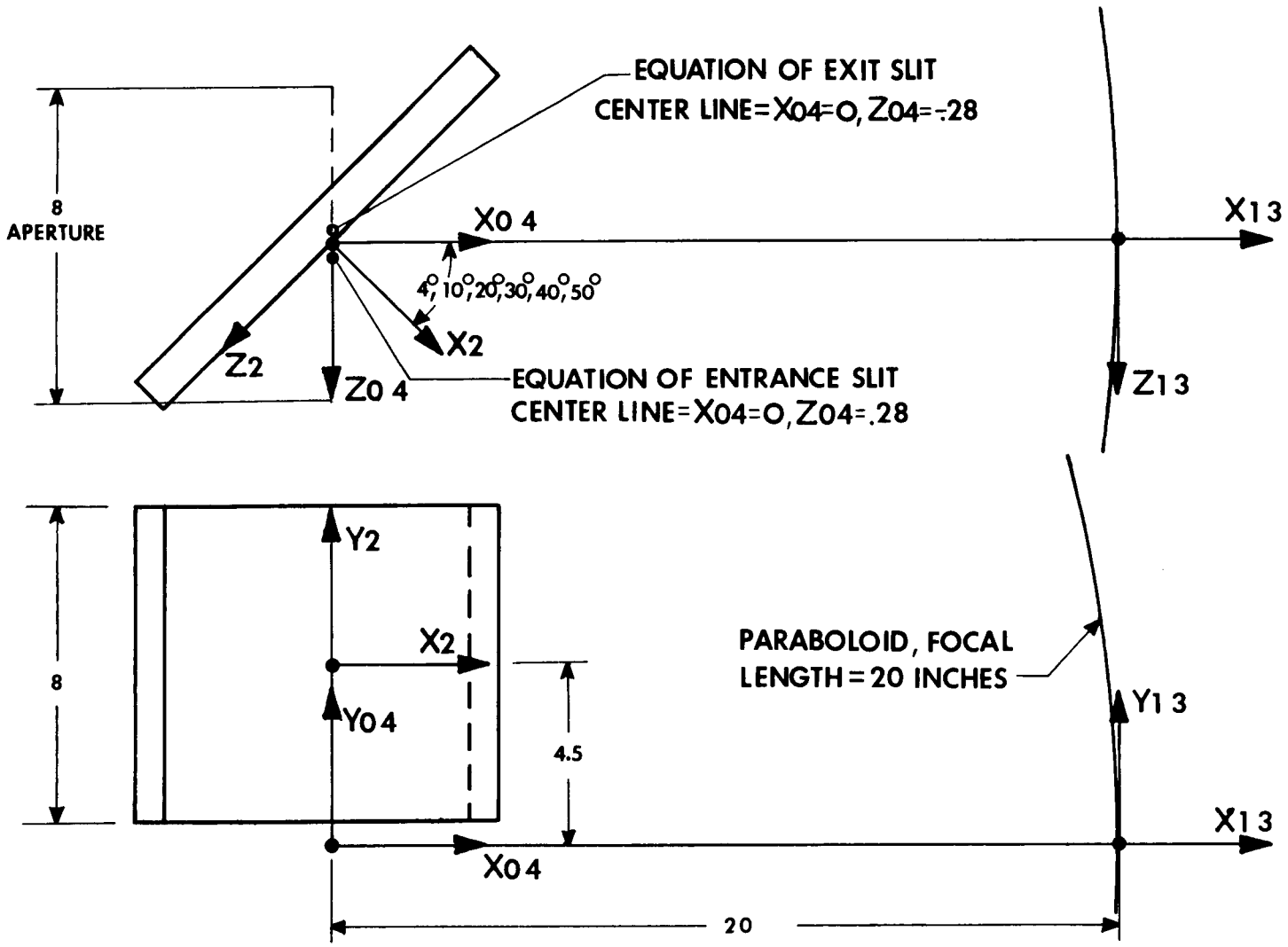

FIG. 1

GEOMETRICAL PRESENTATION OF CALIBRATION MOCHROMATOR

paraboloid as is possible. It is well known that a paraboloid is the ideal reflective surface to form a perfect image from a collimated beam which is parallel to the axis of the paraboloid. This image quality, however, degenerates whenever the collimated beam has an angular deviation from the paraboloid axis. The basic question to ask of this optical system then is how far can the slits be separated and how high can the slits be made and still obtain a usable exit slit image. The required nearness of entrance and exit slits make the Littrow-type monochromator necessary.

There is no good simple optical design for a monochromator with an effective circular aperture of f/2.1 and which requires a fine image quality other than the single paraboloid collimating mirror. There are several high numerical aperture and high quality combination mirror-lens systems that have been developed which do have wide angular fields of use. These are the Schmit mirror-lens system, the Maksutov mirror-lens system, and several other variations of these. However, these systems require lenses which are not appropriate for the broad infrared wavelength ranges required of the calibration monochromator.

2.1.2 Definition of Axis Systems

Because of ray trace demands and for ease of description, all optical configurations have been expressed in terms of a number of three dimensional axes systems. Each optical surface has its own three dimensional axes system. These individual axes systems and their relative positions are defined as follows:

1. All three-dimensional axes systems are right handed as shown at right

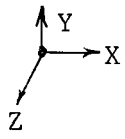

2. For ray tracing the rays commence in the (X0, Y0, Z0) axes system. The first surface encountered by the rays is in the (X1, Y1, Z1) axes system; the second surface encountered by the rays is in the (X2, Y2, Z2) axes system; etc.

3. The location of the origin of the (X1, Y1, Z1) axes system is defined by its coordinate position in the (X0, Y0, Z0) axes system, and it has the coordinate values (A1, B1, C1). The angular orientation of the (X1, Y1, Z1) axes system is related to the (X0, Y0, Z0) axes system by three angles which must be measured in the following order:

   $\alpha 1$ = the rotation of the X1-Z1 plane about the Y1 axis which is held parallel to the Y0 axis. This angle is positive only when the positive X1 axis rotates toward the positive Z1 axis.

   $\beta 1$ = the rotation of the X1-Y1 plane about the Z1 axis after the α 1 rotation is complete. This angle is positive only when the positive X1 axis rotates toward the positive Y1 axis.

   $\gamma 1$ = the rotation of the Y1-Z1 plane about the X1 axis after both the α 1 and $\beta 1$ rotations are complete. This angle is positive only when the positive Z1 axis rotates toward the positive Y1 axis.

Of course, A2, B2, C2, α 2, $\beta 2$, and γ 2 define the (X2, Y2, Z2) axes system in relation to the (X1, Y1, Z1) axes system, etc.

2.1.3 The Calibration Monochromator Axes Systems

Referring to Figure 1 the entrance slit is in the Y0-Z0 plane of the (X0, Y0, Z0) axes system. The entrance slit will be considered to have parallel jaws which are in turn parallel to the Y0 axis. The entrance slit will be placed on the positive Z0 side of the origin.

The collimating mirror is a paraboloid with its apex at the origin of the (X1, Y1, Z1) axes system, and this origin is on the X0 axis at X0 = 20.0 inches. Further, X0 ∥ X1, Y0 ∥ Y1, and Z0 ∥ Z1. The (X1, Y1, Z1) axes system can also be located very simply by the use of the six axes transformation coefficients:

A1 = 20.0	$\alpha 1 = 0$
B1 = 0	$\beta 1 = 0$
C1 = 0	$\gamma 1 = 0$

The focus of the paraboloid is at X1 = -20.0 inches.

The grating surface is the Y2-Z2 plane of the (X2, Y2, Z2) axes system; and may assume one of six different grating incident angles:

A2 = 20.0	$\alpha 2$ = 4°, 10°, 20°, 30°, 40°, and 50°
B2 = 4.5	$\beta 2 = 0$
C2 = 0	$\gamma 2 = 0$

The origin of the (X2, Y2, Z2) axes system is the centroid of the grating surface. The lines of the grating are parallel to the Y2 axis and the grating rotates about the Y2 axis which remains fixed at all times.

The second collimating mirror is the same mirror as the first collimating mirror. Its apex is at the origin of the (X3, Y3, Z3) axes system which is identical to the (X1, Y1, Z1) axes system. Since the same axes system is used as both the first and third axes systems, it is given hereafter the nomenclature (X13, Y13, Z13).

The exit slit is in the (X4, Y4, Z4) axes system which is the same as the (X0, Y0, Z0) axes system and hence shown in Figure 1 as the (X04, Y04, Z04) axes system. The exit slit is parallel to the entrance slit but has a position on the negative side of the Y04 axis.

The neutral axes of the entrance and exit slits have the respective line equations:

Entrance Slit: X04 = 0, Z04 = .28 (inches)

Exit Slit: X04 = 0, Z04 = -.28 (inches)

This represents a slit neutral axes spacing of 2 x .28 = .56 inches.

2.1.4 The Grating Rotation and Its Aperture

The proposed monochromator is a Littrow-type because the entrance slit neutral axis is relatively near (.56 inches for a 20 inch focal length) the neutral axis of the exit slit, and both slit neutral axes are fixed in space. To change the wavelength of light passing through the exit slit, the grating must be rotated about the Y2 axis. During the rotation both the incident and diffraction angles for the light at the grating surface maintain nearly equal values.

The general grating equation is:

$$\frac{N\lambda}{a} = \sin i + \sin\theta \qquad (1)$$

where:

N = grating order

λ = wavelength of light in μ

a = grating line spacing in μ

i = incident angle of light falling on grating surface

Θ = diffracted angle of light from grating surface

To obtain approximate values for the rotational requirements of the grating we can let

$$i = \Theta$$

then substituting in (1)

$$\frac{N\lambda}{a} = 2 \sin i \qquad (2)$$

Note: This approximation cannot be used for the design of the wavelength driving cam of the calibration monochromator to be discussed later. In making the cam calculations it is necessary to use the real values of angles i and Θ .

The grating line spacing can now be stated in terms of the number of lines per mm on the surface of the grating.

$$a = \frac{1000}{k}$$

where:

k = lines/mm on the grating surface

then substituting in (2)

$$\lambda = \frac{2000}{Nk} \sin i \qquad (3)$$

and equation (3) can be written

$$\lambda = K \sin i \qquad (4)$$

where:

$$K = \frac{2000}{Nk} \qquad \text{(a constant)}$$

It is seen then that any grating rotation system is general for all gratings, and any grating drive system which linearizes λ as a function of sin i linearizes λ for any grating K value. Figure 2 is a graphical presentation of λ versus the incident angle i for a number of Nk values for the case where $\Theta = i$. This graph uses logarithmic presentation for the ordinate and abscissa which gives all Nk value curves the same shape. This graph shows the wavelength range that will be obtained for any grating Nk value once the range of i values have been determined for the grating rotation mechanism.

From experience with production spectrophotometers at Beckman, the practical range of i values is generally from about 4° to 50°. For i values greater than 50°, the grating width becomes exceedingly large for retaining the same effective aperture.

2.1.5 Ray Trace Procedure

The purpose of the ray trace of the calibration monochromator is to determine the characteristics of the image of the entrance slit as formed at the exit slit and to determine the exact zones of use for all optical surface. Rather than starting rays from a predetermined entrance slit, rays have been started from representative points on the slit plane which is the Y04-Z04 plane. Figure 3 shows the Y04-Z04 plane and the starting points for the rays used in the ray trace. The coordinates of these starting points are measured in inches in the (X04, Y04, Z04) axes system and are:

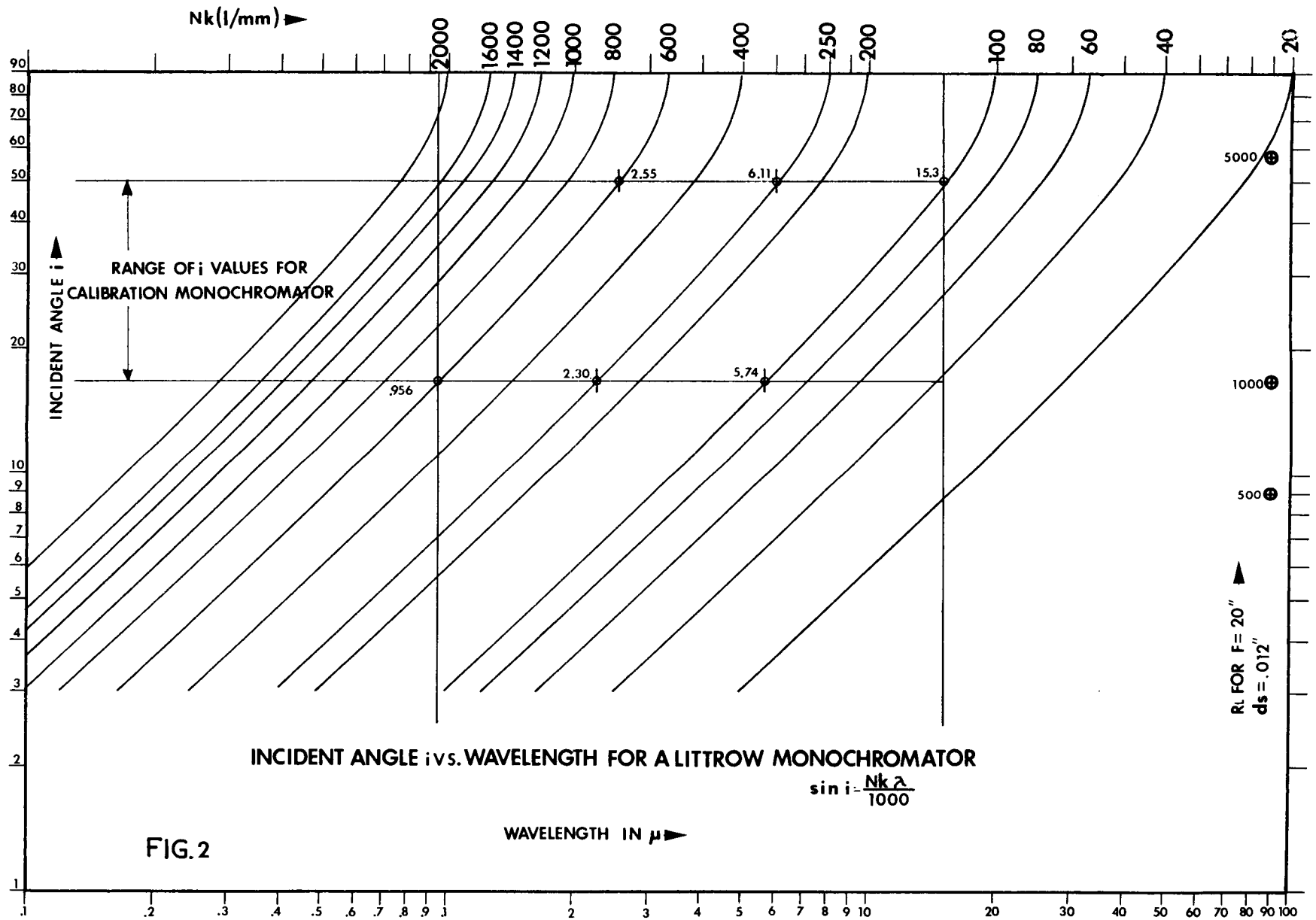
Nk(l/mm)
2000
1600
1400
1200
1000
800
600
400
250
200
100
80
60
40
20
INCIDENT ANGLE i
RANGE OF i VALUES FOR CALIBRATION MONOCHROMATOR
2.55
6.11
15.3
.956
2.30
5.74
5000
1000
500
RL FOR F= 20"
ds = .012"
INCIDENT ANGLE i vs. WAVELENGTH FOR A LITTROW MONOCHROMATOR
sin i = Nkλ/1000
WAVELENGTH IN μ

FIG. 2

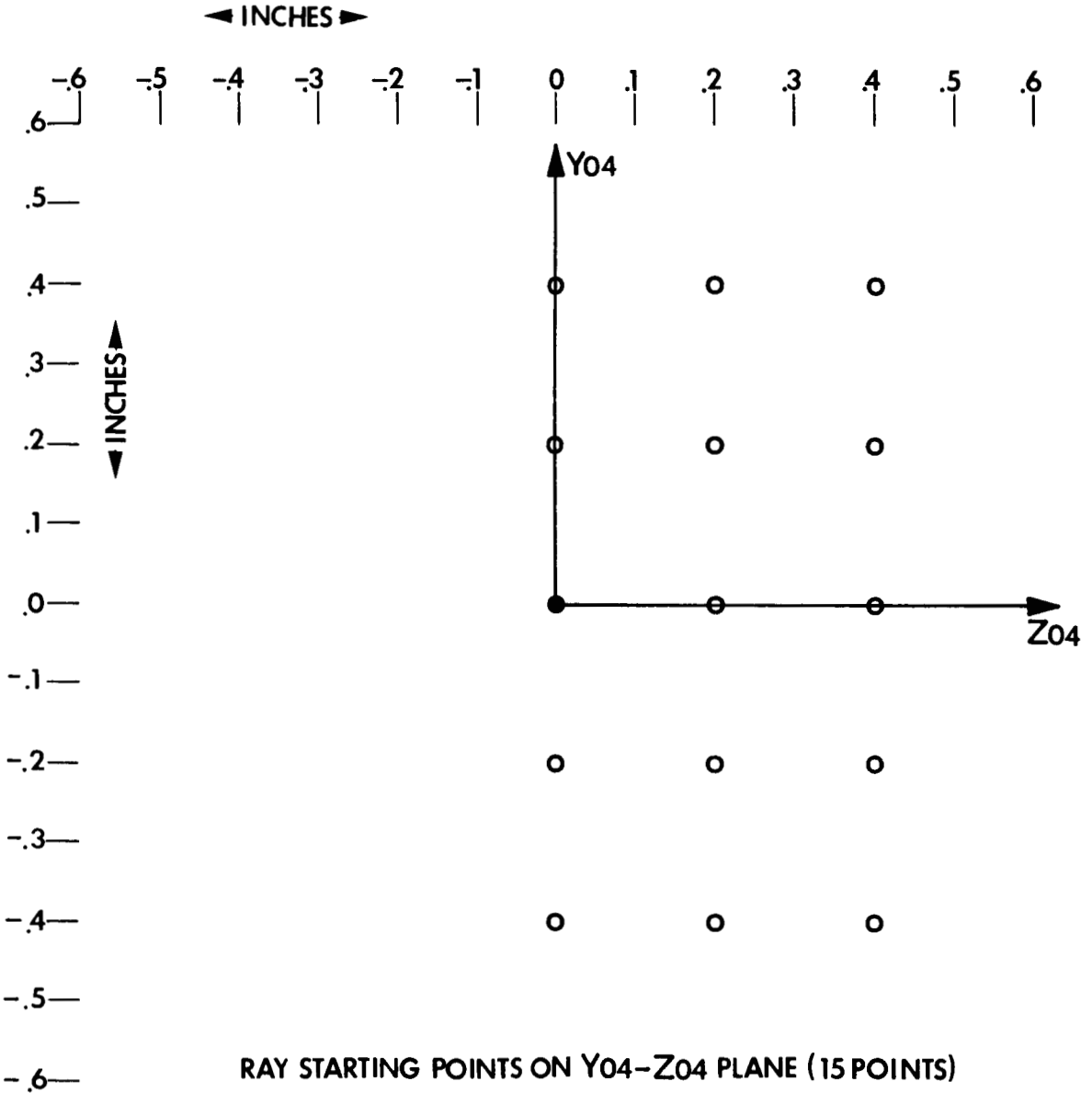

RAY STARTING POINTS ON Y04-Z04 PLANE (15 POINTS)

FIG. 3

(0, .4, 0)
(0, .2, 0)
(0, 0, 0)
(0, -.2, 0)
(0, -.4, 0)
(0, .4, .2)
(0, .2, .2)
(0, 0, .2)
(0, -.2, .2)
(0, -.4, .2)
(0, .4, .4)
(0, .2, .4)
(0, 0, .4)
(0, -.2, .4)
(0, -.4, .4)

These 15 starting points define an area .8 inches (20 mm) high and .4 inches (10 mm) wide on the positive Z04 side of the slit plane. The images of these starting points produced by the monochromator on the Y04-Z04 plane should have precisely the same values as their corresponding Y04 and Z04 starting point values except for being multiplied by (-1). Any differences in the magnitude of these image values are due to optical aberrations. The slit aberration function at any image point on the exit slit plane is defined by the percentage of those rays starting from a single point on the entrance slit plane which fall within given error intervals as measured from the theoretically correct image point. The group of rays so used from a single point must represent rays which form a uniform flux density over the face of the grating.

To accomplish the uniform flux density of rays in the ray trace, 81 rays have been selected for each of the 15 starting points on the entrance slit plane. This gives a total of 15 x 81 = 1215 rays. Each of these 15 sets of 81 rays intersect the grating aperture at identically the same 81 points. Figure 4 is a diagram of the 81 ray positions. These rays form the boundary of the 8 inch square dispersive aperture and form equally spaced columns and rows.

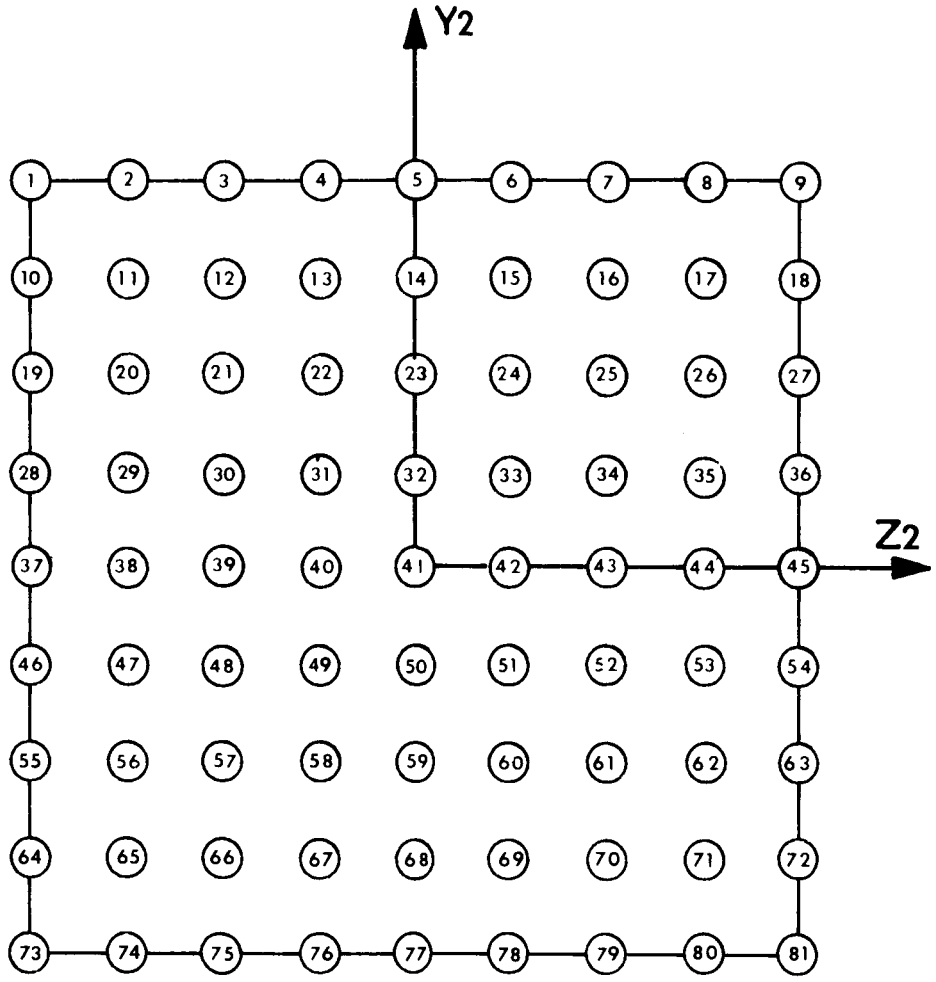

RAY POSITION AT GRATING APERTURE IN Y2-Z2 PLANE WHEN $\alpha = 0^{\circ}$

FIG. 4

The numbers shown are the actual assigned numbers to each ray. The dispersive aperture has been selected to be an 8 inch square in the Y2-Z2 plane, and centered about the origin of the (X2, Y2, Z2) axes system, and it is defined for only the single condition where $\alpha 2 = 0°$, that is where the grating has an incident angle $i = 0°$. It is assumed that an optical stop will be provided outside the monochromator in either the entrance or exit optical systems so that this 8 inch square aperture is always the aperture of the calibration monochromator regardless of the grating rotation.

In selecting a grating to cover this 8 inch square aperture, a grating can be chosen with a height, h = 8 inches as measured along the grating lines. However, the width of the grating measured across the grating lines must have a value equal to or greater than $w = 8/\cos i(\max)$ inches, where i(max) is the maximum incident angle the grating can have in operation.

The complete 1215 rays representing 81 rays from the 15 starting points were actually repeated in the ray trace for 6 different grating incident angles, namely:

$$i = 4°,\ 10°,\ 20°,\ 30°,\ 40°, \text{ and } 50°$$

The diffraction function used in the ray trace program had to be changed for each of the above grating incident angles. The diffraction function is

$$W = \frac{N\lambda}{a} \qquad (5)$$

But by equation (1)

$$\frac{N\lambda}{a} = \sin i + \sin\Theta$$

and for the 5 rays commencing on the Y04 axis, $i = \Theta$ exactly, then

$$W = \frac{N\lambda}{a} = 2 \sin i \qquad (6)$$

W was computed from equation (6) for each of the 6 incident angles used in the ray trace. These W values were then actually used for all 15 ray starting points. The fact that i and Θ are not equal for the 10 ray starting points off of the Y04 axis creates only a negligibly small error in the ray trace analysis.

2.1.6 Results of the Ray Trace of the Calibration Monochromator

2.1.6.1 Aberrations at the Exit Slit Image

For each of the 15 ray starting points on the entrance slit plane, the Y04-Z04 plane, there is an image point on the exit slit plane which is the same Y04-Z04 plane. The ray trace program prints out the X04, Y04, and Z04 coordinates for all 81 rays at each of the 15 image points on the Y04-Z04 plane. Of course all X04 values are equal to zero.

The rays which start from coordinate point (0, 0, 0) will have all 81 rays return to this exact same coordinate point since this is the true focal point of the paraboloid mirror, and there are no aberrations for this point. Rays from all other starting points will exhibit aberration spreads in their Y04 and Z04 values about their ideal image points. The error spread in Y04 values defines the aberrations measured along the direction of the slit height which is at right angles to the monochromator dispersion. The error spread in Z04 values defines the aberrations measured in the direction of the slit width

which is the direction of grating dispersion. The Z04 aberrations reduce the resolution of the monochromator whereas Y04 aberrations cause only some loss of energy.

There are various ways of describing the magnitude and the effect of these aberration spreads at an image point. Three such ways are as follows:

1. The maximum spread in both the Y04 and Z04 values for all 81 rays defines a rectangular area in which the Y04 and Z04 values for all 81 rays lie.
2. Resolution is measured in the direction of dispersion and is usually referred to as half bandwidth which is the width of the slit energy output function between the 50% energy values each side of the maximum energy peak. A synthetic half bandwidth value can be developed from the 81 ray image values for Z04 by using a purely statistical procedure as follows. Slit aberration functions can actually have many shapes, since the shape function depends on the particular optical system forming the image. A simple geometrical shape will be selected here to serve as an approximate slit function. It is the triangle as shown in Figure 5. The half bandwidth of the triangle is the width of the triangle at the half height, or the .5 relative energy level. It is seen that the triangle can then be divided into 8 equal areas as shown. Two of these sections which are cross hatches lie outside of the half bandwidth zone and represent 1/4 the total area of the triangle. Thus, for this triangular function 1/4 of its area is outside of the half bandwidth. If this

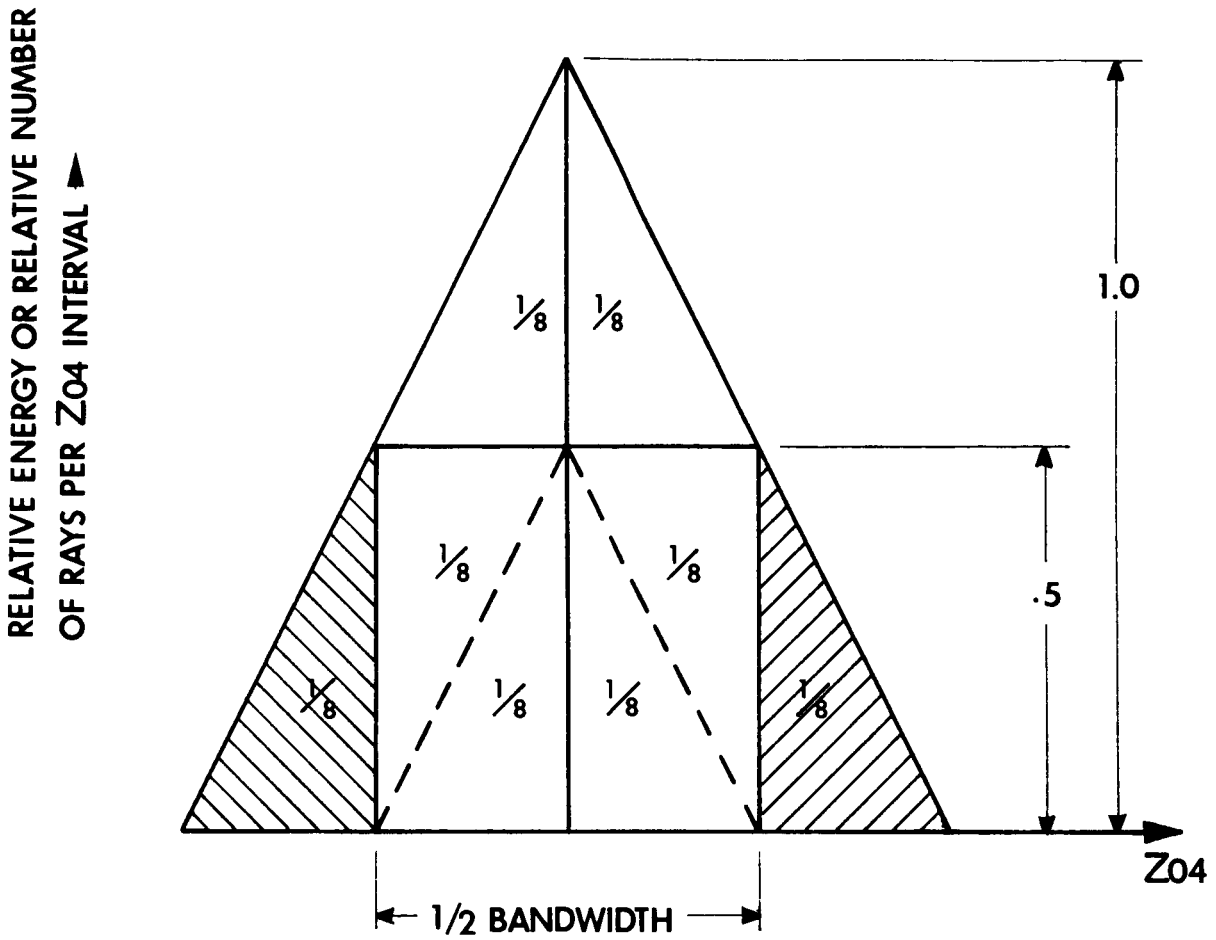

RELATIVE ENERGY DISTRIBUTION FOR
A TRIANGULAR SLIT FUNCTION

FIGURE 5

analogue is used for the 81 rays then 25% or 81/4 = 20 rays will be considered to lie outside of the half bandwidth zone. The 20 rays having the largest error values whether positive or negative should then be deleted and the 61 remaining rays will form the 1/2 bandwidth spread.

3. The third method of defining the aberration is to plot the real slit function and directly measure the band spread at the 50% energy level. This real slit function is a plot of the number of rays which lie in small successive error intervals across the image.

These three methods of image analysis will be used to analyze the ray trace results.

Table I is a tabulation of the image characteristics at the exit slit plane and also at adjacent parallel focusing planes. The image analysis by electronic computer grouped rays into error increments. The error increments used for Y04 values were large (.005 inches) since the image aberrations in this direction are not as important as they are for Z04 errors. The error increments for Z04 values are .001 inches. The first column under the major heading "Image Spread in Inches" is called Δ Z04, and is the required spread in Z04 to include all 81 rays making up the image. The Δ Z04 values are in .001 inch increments so if a value of Δ Z04 = .002, this means that the total image spread is between .001 inches and .002 inches. By studying the size variation of Δ Z04 as a function of the grating incident angle i and the position of the ray starting point in the Y04-Z04 plane, it is seen that the incident angle i has a large effect on the maximum image spread. Δ Z04 is nearly

TABLE I (1)

CALIBRATION MONOCHROMATOR EXIT SLIT PLANE CHARACTERISTICS

i	Ray Starting Coordinates Y04	Z04	Image Spread in Inches ΔZ04	ΔZ'04	Centroid Location in Inches Z04	Z'04	Position of Focus in Inches A4	Span of Focus in Inches ΔA4
	.4	0	.002	.001	-.00040	-.00067	-20.005 to -20.010	.005
	.2	0	.002	.001	-.00013	-.00050	-20.005	-
4°	0	0	.000	.000	.00000	.00000	-20.000	.000
	-.2	0	.002	.001	.00015	-.00049	-20.005	-
	-.4	0	.002	.001	.00001	-.00051	-20.005 to -20.010	.005
	.4	0	.002	.001	-.00079	-.00128	-20.005 to -20.010	.005
	.2	0	.002	.001	-.00004	-.00054	-20.005	-
10°	0	0	.000	.000	.00000	.00000	-20.000	.000
	-.2	0	.002	.001	.00055	.00050	-20.005	-
	-.4	0	.002	.001	-.00082	-.00133	-20.005 to -20.010	.005
	.4	0	.002	.001	-.00216	-.00266	-20.005 to -20.010	.005
	.2	0	.002	.001	-.00023	-.00073	-20.005	-
20°	0	0	.000	.000	.00000	.00000	-20.000	.000
	-.2	0	.002	.001	-.00088	-.00050	-20.005	-
	-.4	0	.002	.001	-.00322	-.00272	-20.005 to -20.010	.005
	.4	0	.002	.001	-.00383	-.00433	-20.010	-
	.2	0	.002	.001	-.00012	-.00121	-20.005	-
30°	0	0	.000	.000	.00000	.00000	-20.000	.000
	-.2	0	.002	.001	-.00067	-.00116	-20.005	-
	-.4	0	.002	.001	-.00380	-.00430	-20.010	-
	.4	0	.003	.002	-.00519	-.00605	-20.005 to -20.010	.005
	.2	0	.002	.002	-.00142	-.00165	-20.005	-
40°	0	0	.000	.000	.00000	.00000	-20.000	.000
	-.2	0	.002	.001	-.00117	-.00167	-20.005	-
	-.4	0	.003	.002	-.00526	-.00609	-20.005 to -20.010	.005
	.4	0	.003	.002	-.00858	-.00908	-20.010	-
	.2	0	.002	.001	-.00193	-.00243	-20.005	-
50°	0	0	.000	.000	.00000	.00000	-20.000	.000
	-.2	0	.002	.002	-.00209	-.00198	-20.005	-
	-.4	0	.003	.002	-.00799	-.00879	-20.005 to -20.010	.005

TABLE I (2)

CALIBRATION MONOCHROMATOR EXIT SLIT PLANE CHARACTERISTICS

i	Ray Starting Coordinates Y04	Z04	Image Spread in Inches ΔZ04	ΔZ'04	Centroid Location in Inches Z04	Z'04	Position of Focus in Inches A 4	Span of Focus in Inches ΔA4
	.4	.2	.001	.001	-.20078	-.20078	-20.010	-
	.2	.2	.001	.001	-.20012	-.20012	-20.005	-
4°	.0	.2	.001	.001	-.19998	-.19998	-20.005	-
	-.2	.2	.001	.001	-.20000	-.20000	-20.005	-
	-.4	.2	.001	.001	-.20027	-.20027	-20.010	-
	.4	.2	.001	.001	-.20161	-.20161	-20.010	-
	.2	.2	.001	.001	-.20068	-.20068	-20.005	-
10°	0	.2	.001	.001	-.20012	-.20012	-20.005	-
	-.2	.2	.001	.001	-.20039	-.20039	-20.005	-
	-.4	.2	.002	.001	-.20135	-.20135	-20.010	-
	.4	.2	.001	.001	-.20323	-.20323	-20.010	-
	.2	.2	.001	.001	-.20120	-.20120	-20.005	-
20°	0	.2	.001	.001	-.20076	-.20076	-20.005	-
	-.2	.2	.001	.001	-.20019	-.20019	-20.005	-
	-.4	.2	.002	.001	-.20270	-.20319	-20.005 to -20.010	.005
	.4	.2	.002	.001	-.20488	-.20538	-20.010	-
	.2	.2	.002	.001	-.20166	-.20216	-20.005	-
30°	0	.2	.001	.001	-.20109	-.20109	-20.005	-
	-.2	.2	.001	.001	-.20191	-.20191	-20.005	-
	-.4	.2	.003	.001	-.20453	-.20533	-20.005 to -20.010	.005
	.4	.2	.003	.001	-.20749	-.20799	-20.010	-
	.2	.2	.002	.001	-.20268	-.20218	-20.005 to -20.010	.005
40°	0	.2	.002	.001	-.20169	-.20169	-20.005	-
	-.2	.2	.002	.001	-.20298	-.20298	-20.005	-
	-.4	.2	.003	.002	-.20706	-.20776	-20.005	-
	.4	.2	.003	.002	-.21029	-.21118	-20.015	-
	.2	.2	.002	.001	-.20414	-.20464	-20.005 to -20.010	.005
50°	0	.2	.002	.001	-.20224	-.20224	-20.005	-
	-.2	.2	.002	.001	-.20438	-.20438	-20.005	-
	-.4	.2	.005	.002	-.21053	-.21107	-20.000 to -20.010	.010

TABLE I (3)

CALIBRATION MONOCHROMATOR EXIT SLIT PLANE CHARACTERISTICS

i	Ray Starting Coordinates Y04	Z04	Image Spread in Inches △Z04	△Z'04	Centroid Location in Inches Z04	Z'04	Position of Focus in Inches A4	Span of Focus in Inches △A4
	.4	.4	.002	.002	-.40125	-.40130	-20.015	-
	.2	.4	.001	.001	-.40076	-.40076	-20.010	-
4°	0	.4	.001	.001	-.40074	-.40074	-20.005 to -20.010	.005
	-.2	.4	.001	.001	-.40029	-.40029	-20.010	-
	-.4	.4	.002	.001	-.40023	-.40023	-20.015	-
	.4	.4	.001	.001	-.40294	-.40294	-20.015	-
	.2	.4	.001	.001	-.40157	-.40157	-20.010	-
10°	0	.4	.002	.001	-.40149	-.40144	-20.005 to -20.010	.005
	-.2	.4	.002	.001	-.40151	-.40083	-20.005 to -20.010	.005
	-.4	.4	.003	.001	-.40173	-.40193	-20.010 to -20.015	.005
	.4	.4	.001	.001	-.40547	-.40547	-20.015	-
	.2	.4	.001	.001	-.40321	-.40321	-20.010	-
20°	0	.4	.002	.001	-.40279	-.40282	-20.005 to -20.010	.005
	-.2	.4	.003	.001	-.40227	-.40324	-20.005 to -20.010	.005
	-.4	.4	.003	.001	-.40449	-.40544	-20.010 to -20.015	.005
	.4	.4	.002	.001	-.40893	-.40890	-20.015 to -20.020	.005
	.2	.4	.002	.001	-.40539	-.40554	-20.010 to -20.015	.005
30°	0	.4	.002	.001	-.40437	-.40433	-20.005 to -20.010	.005
	-.2	.4	.003	.001	-.40521	-.40438	-20.005 to -20.010	.005
	-.4	.4	.004	.002	-.40777	-.40862	-20.010 to -20.015	.005
	.4	.4	.003	.002	-.41268	-.41290	-20.020	-
	.2	.4	.002	.001	-.40808	-.40864	-20.010	-
40°	0	.4	.002	.001	-.40646	-.40639	-20.005 to -20.010	.005
	-.2	.4	.003	.001	-.40782	-.40801	-20.005	-
	-.4	.4	.005	.002	-.41162	-.41273	-20.005	-
	.4	.4	.004	.002	-.41773	-.41859	-20.025	-
	.2	.4	.003	.002	-.41123	-.41154	-20.010 to -20.015	.005
50°	0	.4	.003	.002	-.40890	-.40911	-20.005 to -20.010	.005
	-.2	.4	.004	.002	-.41039	-.41134	-20.005	-
	-.4	.4	.007	.003	-.41685	-.41819	-20.000 to -20.005	.005

3 times larger at i = 50° than at i = 4°. Still the largest maximum image spread encountered is only .007 inches which occurs when i = 50°, Y04 = -.4, and Z04 = .4.

The column to the right of Δ Z04 in Table I is titled Δ Z'04 and refers to a half bandwidth spread determined by deletion of the worst 25% of the rays as described earlier. Again values are in increments of .001 inches and a Δ Z'04 value of .002 inches means that the remaining image spread for the best 75% of the 81 rays is greater than .001 inches and less than .002 inches. It will be noted in Table I that for nearly all cases Δ Z'04 is .001 inches. Only when i = 50° and Z04 = .4 inches is Δ Z'04 predominently .002 inches. It can then be said that the calibration monochromator is capable of producing images with a nominal half bandwidth of .001 inches over the complete image plane for all incident angles up to 40°. At i = 50° the nominal half bandwidth is .002 inches. The Δ Z04 values listed in Table I and similarly the Δ Z'04 values are in each case determined for the plane of best focus. The column of Table I headed A4 gives the positions of the planes of best focus. The rays which start from (0, 0, 0) in the (X04, Y04, Z04) axes system return precisely to this same position and the best focus plane for this one case is the Y04-Z04 plane which has an A4 value of -20.0 inches measured along the X13 axis in the (X13, Y13, Z13) axes system.

All ray starting points other than (0, 0, 0) are by necessity off of the optical axis since the optical axis passes through (0, 0, 0) in the (X04, Y04, Z04) axes system. These off axis starting points will all have image positions with A4 values more negative than -20.00 inches. The more off

the optical axis the ray starting points, the more negative will be the A4 values. This means that the best image plane is actually a sphere touching the Y04-Z04 plane at (0, 0, 0) and concave about the negative X04 axis.

In the A4 column of Table I it will be noted that in some cases there are two A4 values. These two values show the span in A4 distances having the same minimum Δ Z04 value. This span is given in the next column as Δ A4. Computer image analysis was performed only at A4 increments of .005 inches. Thus, A4 and Δ A4 values are in increments of .005 inches.

The entrance slit is to have its neutral axis at Z04 = .28 inches which is part way between the ray starting points at Z04 = .2 and Z04 = .4. From a careful analysis of all Z04 = .2 and Z04 = .4 values it can be inferred that the best position for the exit slit plane should have A4 = 20.007 inches. An alternate and more practical plan is to keep the real entrance and exit slits in a common plane but moved a negative X04 direction from the Y04-Z04 plane -.0035 inches while retaining parallelism with the Y04-Z04 plane.

The Δ Y04 spread was printed out in .005 inch error increments, and for nearly every ray starting condition and every incident angle all 81 rays fell within the .005 inches. Y04 was slightly greater than .005 inches only for Y04 = $\pm$.4 and Z04 = .4 when i = 30°, 40°, and 50°.

Actual exit slit error functions have been plotted for six ray starting points on the Y04-Z04 plane, and for incident angle i = 4°, 20°, and 50°. These 18 curves are shown in Figure 6. The shape of these curves within any .001 inch interval is only extimated since the computer ray trace data

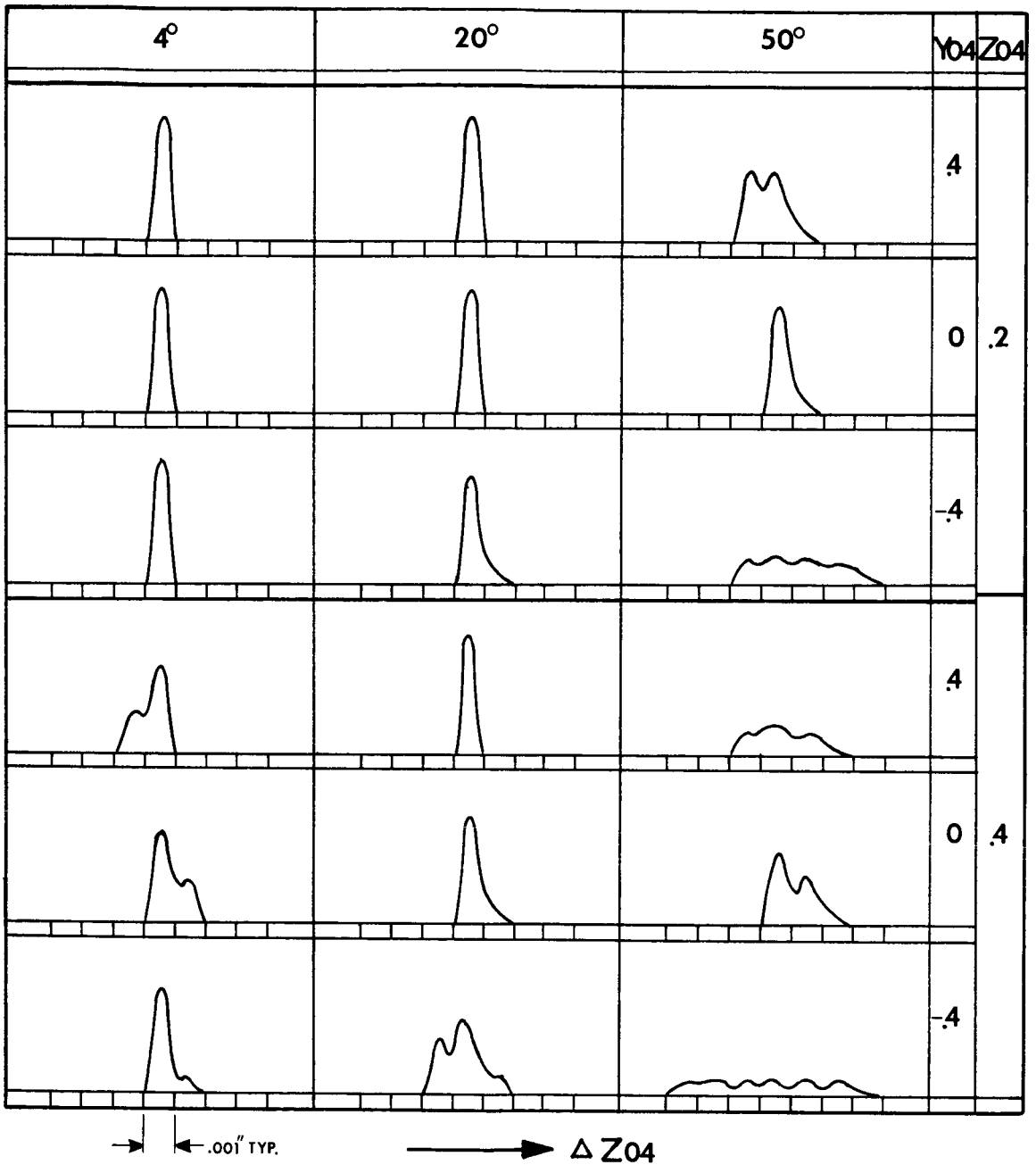

REAL SLIT FUNCTION FOR SIX ENTRANCE SLIT STARTING POINTS AND FOR i VALUES OF; 4°, 20°, AND 50°

FIG. 6

was not analyzed in smaller increments than .001 inch. It is felt that finer analysis is not needed for the subject calibration monochromator.

The interesting thing to observe in looking at these slit functions is that their shapes can vary substantially for different slit starting points. However, in all cases these patterns are narrow relative to the .012 inch (.3 mm) slit width at which resolution performance has been specified in the request for proposal.

2.1.6.2 Slit Curvature

Two columns shown in Table I refer to the image centroid location. These are estimated centroids for the images, but are estimated from an analysis of the computer print out of the rays in each error interval. The Z04 values are the estimated positions of the centroids for images consisting of all 81 rays. The Z'04 values are the estimated centroids for the best 75% of the rays making up the image. The Z'04 values have a more concentrated core and give better centroid values. Let us now observe the differences in magnitude between the Z'04 values in Table I and their respective Z04 starting points at the entrance slit plane. These differences define the so-called slit curvature.

To determine the nature and magnitude of this slit curvature, first, consider the cases when Z04 = 0 for all ray starting points then we find that the centroid position Z'04 is the same for both i = 4° and i = 50° at Y04 = 0. When the ray starting points have Y04 = ±.2 then Z'04 = -.0005 at i = 4°, but at i = 50° Z'04 = -.0024 when Y04 = .2 and Z'04 = -.0020 when Y04 = -.2. When the ray starting points have Y04 = ±.4 then Z'04 = -.0007 when Y04 = .4 and

Z'04 = .0005 when Y04 = -.4 at i = 4°, but for i = 50° Z'04 = -.0091 when Y04 = .4 and Z'04 = -.0088 when Y04 = -.4. These slit image displacements are shown in Table II for the differences in Z'04 between i = 4° and i = 50°. Similar presentation is shown in Table III which is for differences between i = 4° and i = 20°.

Next consider the cases when Z04 = .2 for all ray starting points. We find that for Y04 = 0, Z'04 = -.2000 when i = 4° and Z'04 = -.2022 when i = 50°. This image displacement of -.0022 inches between i = 4° and i = 50° is due to the fact that the incident angle i and the diffracted angle θ were taken to be equal for the ray trace whereas they are actually not with the exception of ray starting points with Z04 = 0. This image displacement error does not affect either the image aberration analysis or the slit curvature analysis if it is handled properly.

For ray starting points at Y04 = ±.2 the change in Z'04 = -.0001 from Y04 = 0 to Y04 = .2 and the change in Z'04 = .0000 from Y04 = 0 to Y0 = -.2 for i = 4°, but for i = 50° the change in Z'04 = -.0024 from Y04 = 0 to Y04 = .2 and the change in Z'04 = -.0022 from Y04 = 0 to Y04 = -.2. For ray starting points at Y04 = ±.4 the change in Z'04 = -.0008 from Y04 = 0 to Y04 = .4 and the change in Z'04 = -.0003 from Y04 = 0 to Y04 = -.4 at i = 4°; but at i = 50° the change in Z'04 = -.0089 from Y04 = 0 to Y04 = .4 and the change in Z'04 = -.0088 from Y04 = 0 to Y04 = -.4. These slit image displacements are also shown in Table II as the Z04 differences between i = 4° and i = 50°.

Finally, consider the cases where Z04 = .4 for the ray starting points. Then

TABLE II

		◄Z04►		
		0	.2	.4
Y04 ▲ ▼	.4	−.0084	−.0081	−.0089
	.2	−.0019	−.0023	−.0024
	0	0	0	0
	−.2	−.0015	−.0022	−.0026
	−.4	−.0083	−.0085	−.0096

SLIT CURVATURE. DISPLACEMENT IN Z_{04} VALUES BETWEEN $i = 4^{\circ}$ & $i = 50^{\circ}$

TABLE III

		◄ Z04 ►		
		0	.2	.4
Y04 ▲▼	.4	-.0020	-.0016	-.0021
	.2	-.0007	-.0003	-.0004
	0	0	0	0
	-.2	0	+.0005	-.0009
	-.4	-.0022	-.0021	-.0031

SLIT CURVATURE. DISPLACEMENT IN Z_{04} VALUES BETWEEN $i = 4^{\circ}$ & $i = 20^{\circ}$

at ray starting point Y04 = 0, Z'04 =-.4007 at i = 4° and Z'04 = -.4091 at i = 50°. Thus the error due to using i = Θ in the ray trace has grown to the difference between the two Z'04 values above or -.0084 inches. The remainder of the analysis for slit curvature at ray starting point Z04 = .4 is identical to that used for Z04 = .2, and the results are shown in Table II.

A similar analysis was performed for i = 4° and i = 20°. These curvature values are shown in Table III.

2.1.6.3 Diffraction Slit Function

The variation in intensity of illumination due to diffraction and measured across the exit slit width of a monochromator, the direction of dispersion, is a function of the focal length of the monochromator and the effective width of the dispersive element. This diffraction function may be expressed by the following equation(1):

$$I = I_o \frac{\sin^2 \beta}{\beta^2} \qquad (7)$$

and

$$\beta = \frac{\pi w \sin \phi}{\lambda} \qquad (8)$$

where:

I_o = intensity of illumination of a given wavelength, λ, falling on the dispersive element.

w = effective width of grating in μ. (measured normal to incident illumination)

λ = wavelength in μ.

ϕ = an angle measured at the dispersive element between the diffracted wave front and the optical axis.

(1) See Fundamentals of Physical Optics, Jenkins and White, Chapter 5.

This equation describes the well-known Fraunhofer diffraction for a single slit, the slit here being the effective width of the dispersive element. This function has a maximum value at $\beta = 0$ and it has zero values at

$$\beta = \pm\pi \ , \ \pm 2\pi \ , \ \pm 3\pi \ \ . \ . \ . \ . \pm n\pi$$

The major portion of energy is in the principle maximum which is positioned between $\beta = \pi$ and $\beta = -\pi$.

This diffraction intensity function can be integrated over the slit aberration function as obtained from ray tracing in order to obtain a precise combined image error function at the exit slit. However, from a practical standpoint, a single number is generally used to describe the diffraction function. This is the diffraction limit or Rayleigh criterion for the diffraction image.

This criterion observes that the diffracted images for two different wavelengths are just distinguishable when the maximum of one diffraction function is over the first minimum of the other, which means the two wavelengths have a diffraction function separation of $\beta = \pi$. Substituting this last relation into equation (8) and calling ϕ , ϕ_r when $\beta = \pi$.

$$\pi = \frac{\pi \, w \sin \phi_r}{\lambda}$$

and

$$\sin \ \phi_r = \frac{\lambda}{w}$$

and for most monochromators and this calibration monochromator in particular ϕ_r is a very small angle and very nearly equal to sin ϕ_r , so finally,

$$\phi_r = \frac{\lambda}{w} \qquad (9)$$

This says that the minimum angular spread between two diffracted wavelengths from the dispersive element which are just resolvable is λ/w.

The crossover point of the two diffraction functions with the $\beta = \pi$ spread is at $\beta = \pi/2$ and substituting this latter value in equation (7)

$$I = \frac{I_o \sin^2 \pi/2}{(\pi/2)^2}$$

$$= \frac{4}{\pi^2} I_o$$

$$= .41 I_o$$

Thus the Rayliegh criterion band spread is measured at the 41% level and this is a slightly wider value than the half energy resolution value which is often used to define the resolution performance of a monochromator, and which was used to define the Δ Z'04 values used earlier in this report.

Let the linear spread of the diffraction limit at the exit slit be S_R, then

$$S_R = F\phi_r$$

where:

S_R = linear spread of the diffraction function in inches, as measured in the direction of the slit width for the case where $\phi = \phi_r$.

F = focal length of monochromator in inches.

Substituting this last equation into equation (9) we have finally

$$S_R = \frac{F\lambda}{w} \qquad (11)$$

The following table gives the results of equation (11) for various values of λ where F = 20.0 inches, and w = 8.0 inches. S_R is given both in inches and mm.

λ (μ)	S_R (inches)	S_R (mm)
1	.0001	.0025
5	.0005	.0125
10	.0010	.0250
15	.0015	.0375

These are very small diffraction values for an infrared spectrophotometer. This is because of the large numerical aperture of the optics. It should be noted that in equation (11), F/w is equal to f/number when F and w are in the same units. Thus S_R is directly proportional to f/number.

It is seen from the table that the maximum diffraction image spread which occurs at 15μ is only .0015 inches, and this value is very close to the average image abberation spread at the exit slit. Thus, this monochromator has an excellent match between aberrations and diffraction and at no wavelength is the monochromator diffraction limited. Most commercial infrared monochromators are diffraction limited for wavelengths greater than 5μ.

2.1.6.4 Resolving Power, Resolution, and Linear Dispersion

Resolving power, resolution, and linear dispersion of a grating monochromator such as the calibration monochromator under study can be derived from the general grating equation (1). Each of these three terms requires a determination of the rate change in the wavelength value as a function of its image

position measured across the exit slit width.

For any given wavelength imaged at the center of the exit slit, there is a given incident angle i. We are interested in determining the rate change of this wavelength value about this angle i. This change is described by changes in angle Θ while holding angle i constant. Differentiating equation (1) with respect to λ and Θ we have

$$\frac{N}{a} d\lambda = \cos \Theta \, d\Theta$$

and

$$d\lambda = \frac{a \cos \Theta}{N} \, d\Theta \qquad (12)$$

Now if an incremental distance across the exit slit width measured in inches is ds, then

$$d\Theta = \frac{ds}{F} \qquad (13)$$

where:

F = focal length of monochromator in inches.

and

$$d\lambda = \frac{a \cos\Theta}{NF} \, ds \qquad (14)$$

The definition of resolving power is

$$R = \frac{\lambda}{d\lambda}$$

so

$$R = \frac{\frac{a}{N} (\sin i + \sin \Theta)}{\frac{a}{NF} \cos \Theta \, ds}$$

$$R = \frac{F(\sin i + \sin \Theta)}{\cos \Theta \; ds} \qquad (15)$$

For the Littrow monochromator wherein angles i and Θ are nearly equal, such as is the case with the calibration monochromator, we can write

$$i = \Theta$$

and then

$$R_L = \frac{2F \sin i}{\cos i \; ds}$$

and finally

$$R_L = \frac{2F \tan i}{ds} \qquad (16)$$

where R_L is the resolving power of a Littrow monochromator. Equation (16) is general and shows that resolving power is a function only of the focal length of the monochromator, the incident angle of the grating, and the slit width ds. Figure 7 shows the R_L values versus incident angle i for the calibration monochromator with a focal length of 20 inches and for various ds values. In Figure 2, along the right hand ordinate, have been listed the R_L values which correspond to the incident angle i for the case when F = 20 inches and ds = .012 inches (.3 mm). The ds value of .005 inches which is also shown in Figure 7 is a good estimate of a reliable and repeatable minimum image half bandwidth. Thus these resolving power values show the capabilities of this monochromator at small slit widths.

By resolution of the monochromator is meant its ability to separate one wavelength from another. If the slit function is a triangular function as it is when the slit width is much greater than the combined diffraction and aberration half bandwidth, then two wavelengths are just resolved when the two

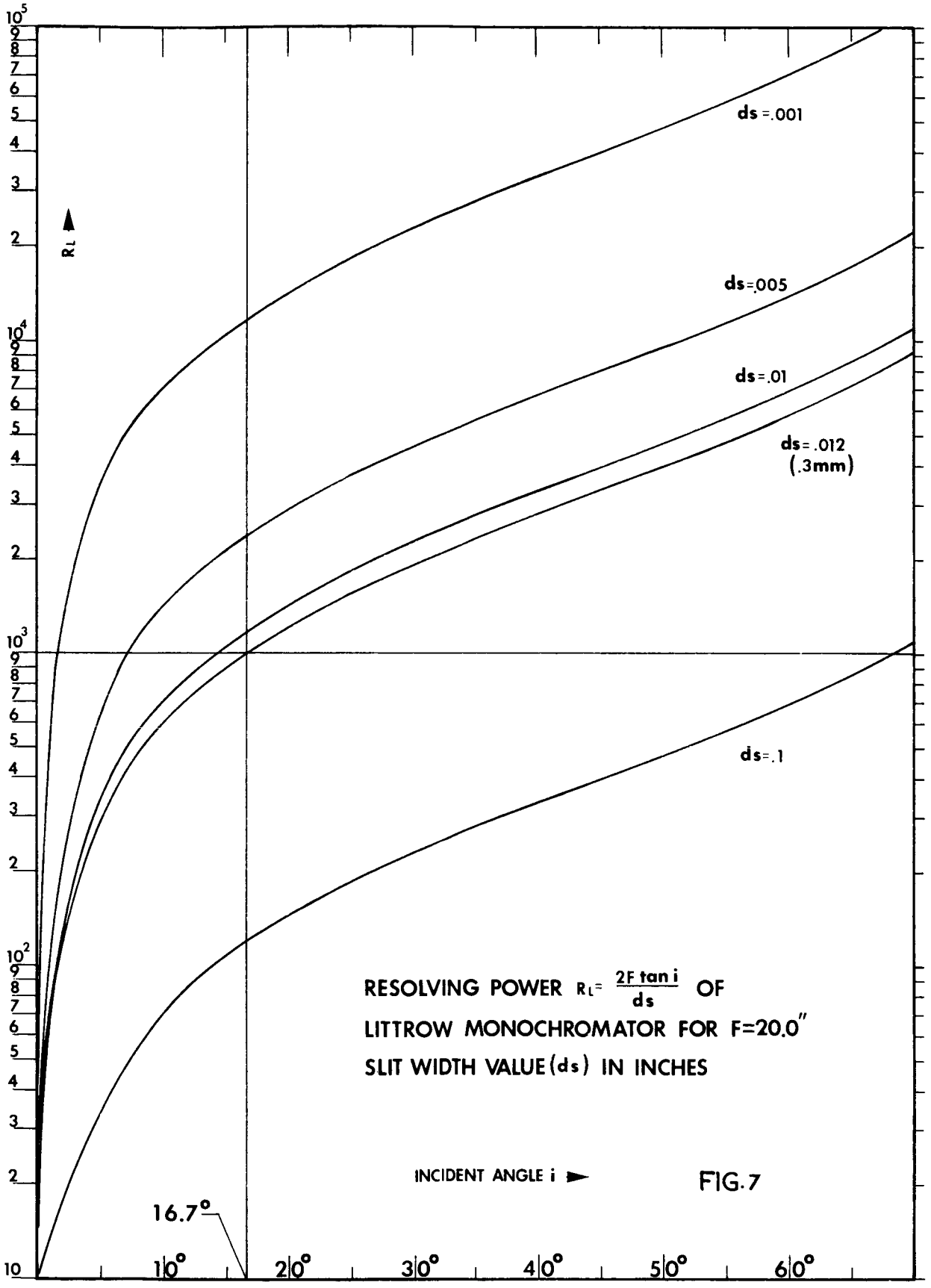
10^5
10^4
10^3
10^2
R_L
ds =.001
ds=.005
ds=.01
ds=.012
(.3mm)
ds=.1
RESOLVING POWER $R_L = \frac{2F \tan i}{ds}$ OF
LITTROW MONOCHROMATOR FOR F=20.0"
SLIT WIDTH VALUE (ds) IN INCHES
INCIDENT ANGLE i
16.7°
10°
20°
30°
40°
50°
60°

FIG.7

wavelengths have a linear separation equal to the slit width ds. Equation (14) is then the resolution function and it can also be written

$$d\lambda = \frac{2000 \cos \Theta}{NkF} \quad ds \tag{17}$$

Since in this monochromator the diffraction angle Θ will have approximately the same magnitude as the incident i, equation (17) becomes

$$d\lambda = \frac{2000 \cos i}{NkF} \quad ds \tag{18}$$

Now the value of angle i will probably not cover a greater range than i = 4° to i = 50°, and

cos 4° = .998

cos 50° = .643

It is seen then by equation (18) that for a given slit width, ds, the resolution, $d\lambda$, can be only 65% as large when i = 50° as it is when i = 4°. This shows that the resolution of a grating is not constant with wavelength.

The linear dispersion at the exit slit is defined as the incremental distance across the exit slit width for an incremental wavelength. From equation (18) we have

$$\frac{ds}{d\lambda} = \frac{NkF}{2000 \cos i} \tag{19}$$

and its units are inches/μ.

2.1.7 Grating Selection

In the appendix of this report will be found the Technical Discussion portion of the Beckman Instrument's technical proposal to JPL for the calibration monochromator study contract. This technical proposal has been included

since Pages 2-1 to 2-10 discuss and illustrate the performance of one, two, and three grating monochromator systems. The conclusion of this analysis is that three separate gratings each used in the first order are required to properly cover the 1 to 15μ wavelength region. The analytical approach to selection of a grating which is to follow will assume that three separate gratings are used in their first order only. It is further assumed that each grating will be provided with prealigned mounting facilities which will allow rapid manual interchange of gratings.

The Request for Proposal has specified that the wavelength range of the monochromator is to be from 1μ to 15μ and that the resolving power is to be 1000 when the slit width is .3 mm (.012 inches). Figure 7 is a graphical presentation of resolving power versus the grating incident angle for a Littrow monochromator which is the same type monochromator as the calibration monochromator proposed here. This particular graph has been plotted for the design parameters of this calibration monochromator, that is the focal length F= 20 inches. As shown in Figure 7 and also as computed using equation (16) the incident grating angle for a resolving power R_L = 1000 and a slit width ds = .012 inches is

$$\tan i = \frac{R_L \, ds}{2F}$$

$$= \frac{1000 \times .012}{2 \times 20} = .3$$

$$i = 16.70°$$

The grating of this monochromator must always have an incident angle equal to or greater than 16.70° in order to maintain the resolving power of 1000. This 16.70° incident angle is shown as a horizontal line in Figure 2. The calibra-

tion monochromator must be operated above this 16.70° line at all times.

A second horizontal line has been drawn on the graph of Figure 2 at an incident angle i = 50°. It will also be seen from Figure 2 that as i goes to greater angles than 50° the dispersion increases rapidly, but very little wavelength range is added. The actual range of incident angles to be used will then be from 16.70 to 50°. In Figure 2 along the right ordinate is shown the resolving power values for F = 20 inches and ds = .012 inches (.3 mm).

A single cam can now be designed which will drive any grating, regardless of Nk value, from i = 16.7° to i = 50° such that the wavelength, λ, passing through the exit slit of the monochromator will be a linear function of angular cam rotation. This cam design will be discussed later in greater detail.

Figure 2 shows a number of Nk value curves to facilitate the selection of the best gratings for any wavelength range. Gratings will only be used in their first order in this monochromator, thus N = 1, and the Nk curves become just k value curves and give the lines/mm of the grating directly. The three best grating k values for the 1μ to 15μ range are 100 lines/mm, 250 lines/mm, and 600 lines/mm.

These three are shown in Figure 2 and it may be seen that these three gratings give excellent wavelength overlap characteristics. The following table shows the usable wavelength range of these three gratings:

k	λ(i = 16.7°)	λ(i = 50°)
600 lines/mm	.956μ	2.55μ
250	2.30	6.11
100	5.74	15.3

If the blaze wavelengths are properly selected for these three gratings, their grating efficiences will be 50% or better over their respective wavelength ranges. Figure 8 shows the approximate energy distribution of the three gratings and the optimal selection of blaze wavelength. These best blaze wavelengths are as follows:

k	Blaze Wavelength	Blaze Angle
600 lines/mm	1.4μ	25.0°
250	3.4μ	25.0°
100	8.5μ	25.0°

It will probably be difficult to find standard or ready made gratings for this monochromator. If new gratings must be ruled then they should be made as specified above. It will be noted that all have the same blaze angle of 25°.

2.1.8 Wavelength Cam vs. Lead Screws

The grating is to be rotated about the Y2 axis which is a fixed axis in the monochromator, and the grating must also be mounted on a bearing system the axis of which is parallel to both the lines of the grating and the Y2 axis. As described in the previous section of this report, the grating is to be rotated through an angular range of 33.3° which changes the grating incident

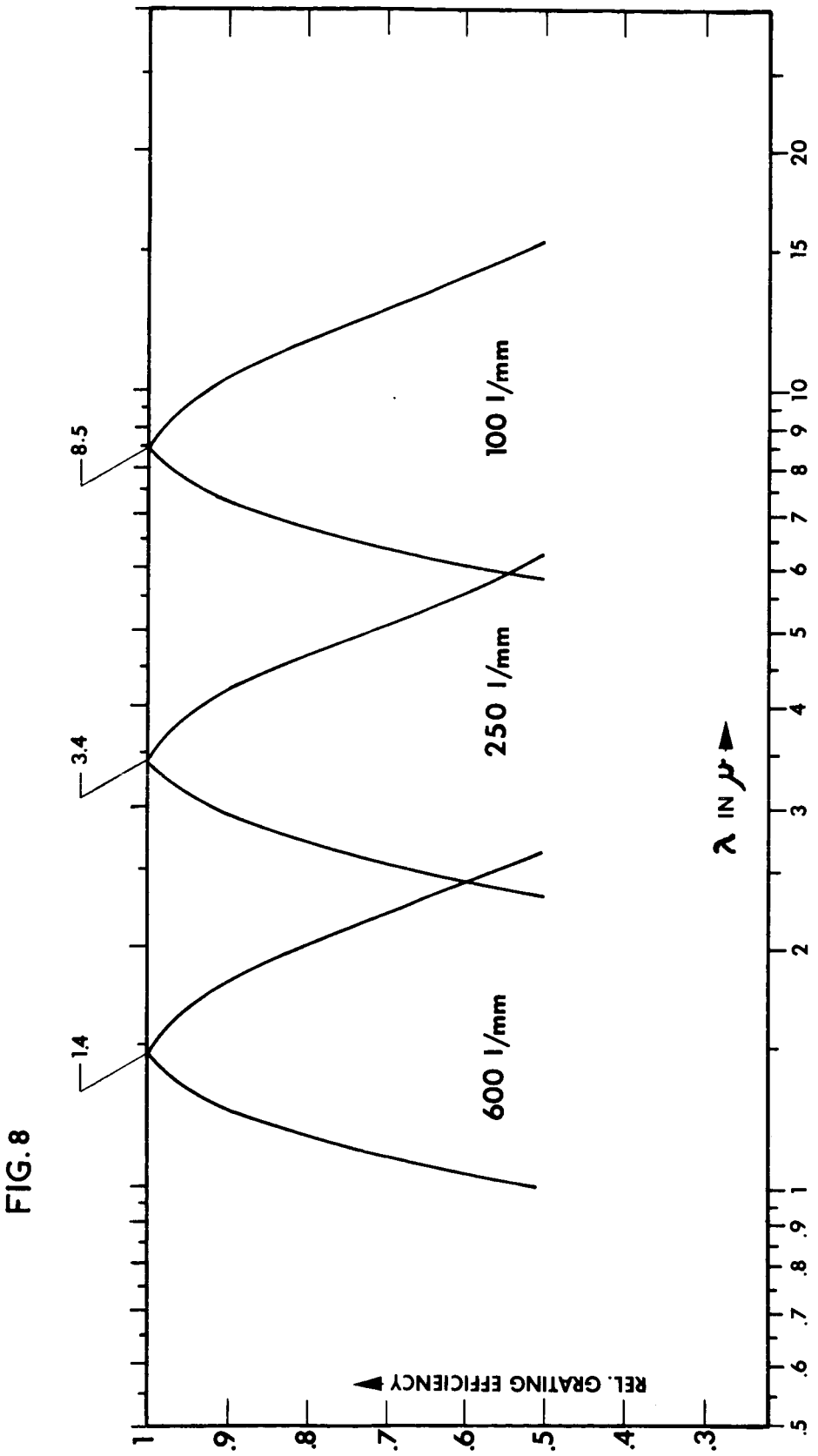

FIG. 8

RELATIVE GRATING EFFICIENCY FOR 3 OPTIMAL BLAZE CONDITIONS

angle from 16.7° to 50°.

The two mechanisms which have been generally used to control the angular position of gratings have been the lead screw and the cam. A lead screw is a highly precision linear screw with matching nut unit and it has found use in many monochromator designs. If the monochromator is a Littrow-type and $i = \Theta$ then it can be seen by the equation (2) that

$$\lambda = \frac{2a}{N} \sin i$$

where:

$2a/N$ = a constant

λ is then a linear function of sin i. In operation the lead screw serves as one side of a right triangle; the side opposite to angle i. The hypotenus of this triangle is maintained at a fixed length; one end being fixed to the grating axis of rotation and the other end attached to the lead screw nut through a freely rotatable bearing. The end of the lead screw opposite the nut must be allowed to slide along a third axis fixed to the monochromator structure and also passing through the rotating axis of the grating. The lead screw must always be at right angles to this fixed axis. This lead screw and linkage system will then linearize wavelength output as a function of lead screw rotation. The lead screw, however, has a number of disadvantages:

1. It correctly linearizes wavelength only when $i = \Theta$.
2. It is difficult to linearize wavenumber $(1/\lambda)$ when this is needed.
3. The linkage mechanism is complex requiring both rotating and sliding bearings with very little clearance.

4. Under operating conditions in a vacuum and over severe temperature cycles, this mechanism would be subject to binding and erratic operation.
5. Errors caused by large temperature changes would be indeterminate because of unknowns in the temperature transfer characteristics of the structure.

The cam, on the other hand, has become a very popular device recently for control of the gratings. It was not too many years ago that it was very expensive to calculate and machine a really high quality cam.

The recent development of electronic computers and ultra high precision jig borers have made the construction of precision cams economically feasible. The cam has many advantages as a grating control:

1. Cams can be made to almost any mathematical function.
2. Interchangeability of cams is simple since they are supported on a single rotatable bearing axis which is fixed to the monochromator structure.
3. More than one cam can be mounted on a common axis shaft to accomplish several precision tasks simultaneously.
4. The cam has a single axis bearing system which is simple and dependable. There is a sliding or rolling contact produced by the cam follower which is a fixed part of the grating mount, but this contact pressure can usually be kept very low so the sliding or rolling friction is very small.
5. The performance of the cam system with changes in temperature is computable and predictable because of the structural simplicity.

2.1.9 Wavelength Cam Design

There are two general methods of using cams to control a grating.

1. The first system uses a circular follower. The actual cam follower is either a fixed cylinder or sphere; or the outer race of a ball bearing. The fixed followers are used when contact pressures between the follower and the cam are very low. At high contact pressures the ball bearing is usually necessary.

   In this type of cam control, the follower is mounted to the grating support and the distance between the center of the circular follower and the axis of the grating is usually called the wavelength arm length. In calculating the cam shape, the cam shape function is usually calculated for the center of the follower. Then by cutting the cam with a machine tool of precisely the same diameter as the follower, the cam is given the correct shape without making corrections for the follower radius in the mathematical equations.

2. In the second system of cam control the follower is a flat plane which lies tangential to the cam shape. In this system the effective wavelength arm length is variable. Also it is the first differential of the cam-grating function which must be derived and solved simultaneously with the angle of attack of the flat plane follower.

Both of the above cam control systems must make use of the same grating rotation function. This function is derived directly from the general grating equations (1) and (5)

$$W = \frac{N\lambda}{a} = \sin i + \sin \Theta$$

When the entrance and exit slit are fixed relative to one another as is the case here, then Θ and i are always different by a small constant angle which will be called j; thus

$$\Theta = i + j \qquad (20)$$

then

$$W = \sin i + \sin (i + j)$$

The last term in the above equation can be expanded. Both sides of the equation are then squared and, finally, terms in i and j are collected separately. The result is

$$\sin i = \frac{W}{2} + \sqrt{\frac{W^2}{4} - \frac{W^2 - \sin^2 j}{2(1 + \cos j)}} \qquad (21)$$

This equation expresses the value of i for any wavelength value. It should be realized that

$$i = \alpha 2$$

where $\alpha 2$ is the angle of rotation of the X2-Z2 plane about the Y2 axis as shown in Figure 1.

It should be noted that if j = 0, which means that $i = \Theta$, then equation (21) reduces to

$$\sin i = \frac{W}{2}$$

which is equation (2) and which was used in the ray trace and was exact only when rays started on the Y04 axis.

In the case of the calibration monochromator, the entrance and exit slit

neutral axes are separated by .56 inches and angle

$$j = 0° - 2' - 20''$$

This j value and equation (21) should be used in any cam calculations. To use equation (21) in a cam calculation it is necessary to substitute for λ in the equation with a term which describes the relation of λ to the angular position of wavelength readout scale values. The readout scale should be a part of the cam or a linear gear ratio of it, if a gear system is involved between the readout and the cam.

The variations in both the mechanical linkages and the dimensions of the cam control system determine the relationship of i and the cam readout angle, and since there are several different orientations for the cam and follower which change the signs and the order of terms, no equations will be developed here. The exact cam and follower arrangement has not been determined as a part of this study.

2.1.10 Allowable Tolerances in Construction Dimension

In a monochromator there are ideal dimensions for all optical elements and also ideal mounting positions for them which are required to produce a spectral image at the exit slit of the monochromator which has the exact wavelength defined by the wavelength readout, and also has the least possible half bandwidth spread for the particular monochromator optical configuration. Minimum half bandwidth image spread and absolute wavelength accuracy have real meaning only when the slit width is reduced to the magnitude of the combined diffraction and aberration spread. The match between the slit image curvature and the

actual slit curvature will affect wavelength accuracy over and above the effects due to diffraction and aberration bandwidth spread.

An analysis of Table I will show that the half bandwidth image spread due to aberrations would be less than .001 inches for nearly all conditions at a ray starting point of Z04 = .28 inches, which is the entrance slit position. This fact is determined by interpolation of the image characteristics for ray starting points at Z04 = .2 and 04 - .4. It should be noted that we are discussing half bandwidth spread, Δ'Z04, and not maximum spread, Δ Z04.

As we also have seen from the section which discussed the diffraction image, the maximum diffraction half bandwidth occurs at the upper wavelength limit which is 15μ and this half bandwidth is .0015 inches. This same diffraction spread at 1μ is only .0001 inches. Thus if the monochromator is properly focused the half bandwidth spread due to the total effects of aberrations and diffraction will be less than .0025 inches at 15μ and less than .0010 inches at 1μ.

Referring to Table II and Table III, it is seen that the so-called slit curvature is a Z'04 displacement which is zero when Y04 = 0, and increases for both positive and negative Y04 values. This Z'04 displacement is also very nearly zero for all ±Y04 starting points when i = 4°, but it increases rapidly at large values of angle i. Table II and Table III show the Z'04 displacements which occur for i = 50° and i = 20° respectively. The average slit curvature displacements are seen to have approximately values of -.0085 inches at the slit starting point Y04 = .4, Z04 = .28 and -.0090 inches at

at Y04 = -.4, Z04 = .28 when i = 50°. Similarly, the average slit curvature displacement when i = 20° is seen to be approximately -.0020 inches at Y04 = .4, Z04 = .28 and -.0024 inches at Y04 = -.4, Z04 = .28. The slit is usually given curvature by constructing a circular slit jaw edge which passes through both the zero displacement point on the Z04 axis, and the displacement coordinate point where Y04 = ±.4. The slit curvature selected will also usually lie between the extreme values. For this monochromator the extreme values occur for angle i = 16.7° and i - 50° and have, respectively, the approximate displacements of -.0018 and -.0085 for Y04 = .4, and -.0020 and -.0090 for Y04 = -.4. The negative Y04 starting points have images with slightly more slit curvature displacement than the positive values. This is probably due to coma. The i = 16.7° values have been interpolated from the i = 4°, 20°, and 50° values.

Finally the, the average slit curvature displacement will be taken to be -.0050 when Y04 = ±.4, Z04 = .28. This is satisfied by a circle with a 16.0 inch radius. The same curvature will be used here for both positive and negative values of Y04. This slit curvature may be applied to either the entrance or exit slit of the monochromator. In the case of the calibration monochromator under study here, the exit slit will be kept straight and the entrance slit will be given the curvature. With the use of this average slit curvature value the maximum image curvature displacements will occur at the two ends of the slit, and at the wavelengths of 1μ and 15μ. The maximum magnitude of these displacements are only .0040 inches. This is still much smaller than the .012 inch (.3 mm) slit width for which resolving power was

specified in the design specifications. In fact, it is seen that the total of all slit image errors including curvature can be held to below .005 inches for the full wavelength range and at this slit width the resolving power of the monochromator will be 2.5 times its value at a .3 mm slit width. In Figure 7 one of the curves shows a resolving power of the monochromator versus wavelength for a slit width of .005 inches.

The aberration function, however, is not necessarily always a small value. We have been considering its value when the monochromator is in focus. A slight defocus will enlarge the aberration spread at the exit slit very suddenly. As in any optical system, the depth of focus is much shorter when the optics have a high numerical aperture, as in the case of this calibration monochromator.

The calibration monochromator has a focus length of 20 inches and an aperture in both the Y2 and Z2 directions of 8 inches. Thus any point at the exit slit when the exit slit is in focus is the apex of a system of rays which form a four sided pyramid with an 8 inch square base and a height of 20 inches. Therefore, if the slit is defocused by moving it along the axis of the pyramid away from the apex, then the aberration spread will increase in both the Y04 and Z04 directions at a rate of 8 inches for moving 20 inches along the pyramid axis. More realistically we can say that if the slit is moved .020 inches from the apex of the pyramid along the height axis of the pyramid then the aberration spread is .008 inches which is 2/3 of a .3 mm slit width. It should be realized also that this pyramid geometry doesn't hold in a region with ±.005 inches of the apex due to aberration and diffraction spreads.

A monochromator of this quality and expense should be focused to within .005

inches of the ideal apex value. This can best be accomplished by placing tolerances on the design of the monochromator and optical parts so that the total displacement of the apex at the slit when assembled is no greater than .040 inches. The slits should then be constructed in such a way that they can be aligned and mounted on the apex within an accuracy of .005 inches. Positioning the slit at the focus can be accomplished by visually looking into the exit slit at the grating face. The entrance slit must at the same time be illuminated with light from a low pressure mercury source, and this same light must fill the grating. The grating is then rotated until it is seen to be filled with green light. This occurs when one of the grating orders for the 546 mm line of mercury pass through the exit slit. Next the slits are narrowed to a .001 inch slit width. Some areas of the grating will remain green, but other areas will become dark. The bright areas are those areas which have rays that pass through the exit slit. Rays from the dark areas have been stopped by the exit slit jaws. When the slits are out of focus only a narrow vertical zone of the grating will be green, and this area will move laterally across the face of the grating whenever it is rotated. When the slits have been moved into the best focal plane, nearly the full grating will be illuminated uniformly. (Table II shows that the best focusing can be done at the shorter wavelength end of the wavelength range where angle i values are smallest. It is seen in this table that not all rays are actually contained with a .001 inch spread. Also, best focus image will be aided by only using the central part of the slit height.) If the grating is now rotated only very slightly the full grating face will be plunged into darkness almost immediately over all parts of the grating face simultaneously.

The above method can position the slit within .005 inches of the best focus if the slit width used for focusing is .001 inches. Still more precise focusing can be achieved by further narrowing of the slits, and then looking for the shadow patterns on the face of the grating which are functions of the Z04 errors at the focus for each zone of the grating, and can be determined from the ray trace data. Focusing with the .001 inch slits will give ample performance for this monochromator requirements.

2.1.10.1 Mirror Support Surfaces

If now the intent is to allow the total error build up in the monochromator to be .04 inches and then correct this by visual positioning of the slit system, then the errors in machining the monochromator structure and the errors in the focal length of the collimating mirror can add up to only .040 inches. In order to mount the collimating mirror, portions of its paraboloid optical surface should be used for direct mounting in contact with matching machined surfaces on the monochromator structure. Such mounting surfaces on the monochromator structure can be machined if it is remembered by geometrical analysis that all planes which are normal to the axis of a paraboloid of revolution, and which intersect the paraboloid have an intersection which is a circle. For any of these circular intersections a cone can be defined which is in contact with the circle and tangential to the paraboloid. Next consider only a frustum of this tangential cone with a total height of .040 inches say, having equal height above and below the circle of contact. Such a frustum of a cone will match the paraboloid very closely.

Modern machine tools such as jig borers and job mills can machine such a frustum of a cone with very high positioning accuracy. Of course, only sectors of such surfaces are required, if such sectors will support the paraboloid with absolute stability.

Figure 9 shows the areas of the paraboloid collimating mirror which are used as both the first and the third surfaces of the monochromator. The conical section mounting surfaces must be outside of this area of us. Figure 9 shows 4 conical sections but made from sections of only two different frustum of cones.

Each circle of contact and frustum of a cone must have the X13 axis its own axis. The small machined conical areas should be located to within ±.001 inches of their theoretical locations. Any errors in locating these surfaces will cause one or both of the following image errors at the exit slit.

1. Errors in X13 position of the conical surfaces produce an X04 error at the exit slit which will have a magnitude which is twice the size of the X13 position error.
2. Errors of different magnitude and sign in the relative positions of the machined areas will cause the collimating mirror axis to be tilted from the ideal paraboloid axis. The component of this error measured in the X13-Y13 plane may cause errors up to a maximum possible error displacement in the Y04 image position of .005 inches which represents only a .6% loss of energy due to .6% of the energy falling above or below the exit slit. The component of this error measured in the X-13-Z-13 plane will cause a maximum Z04 error at the exit slit of .005

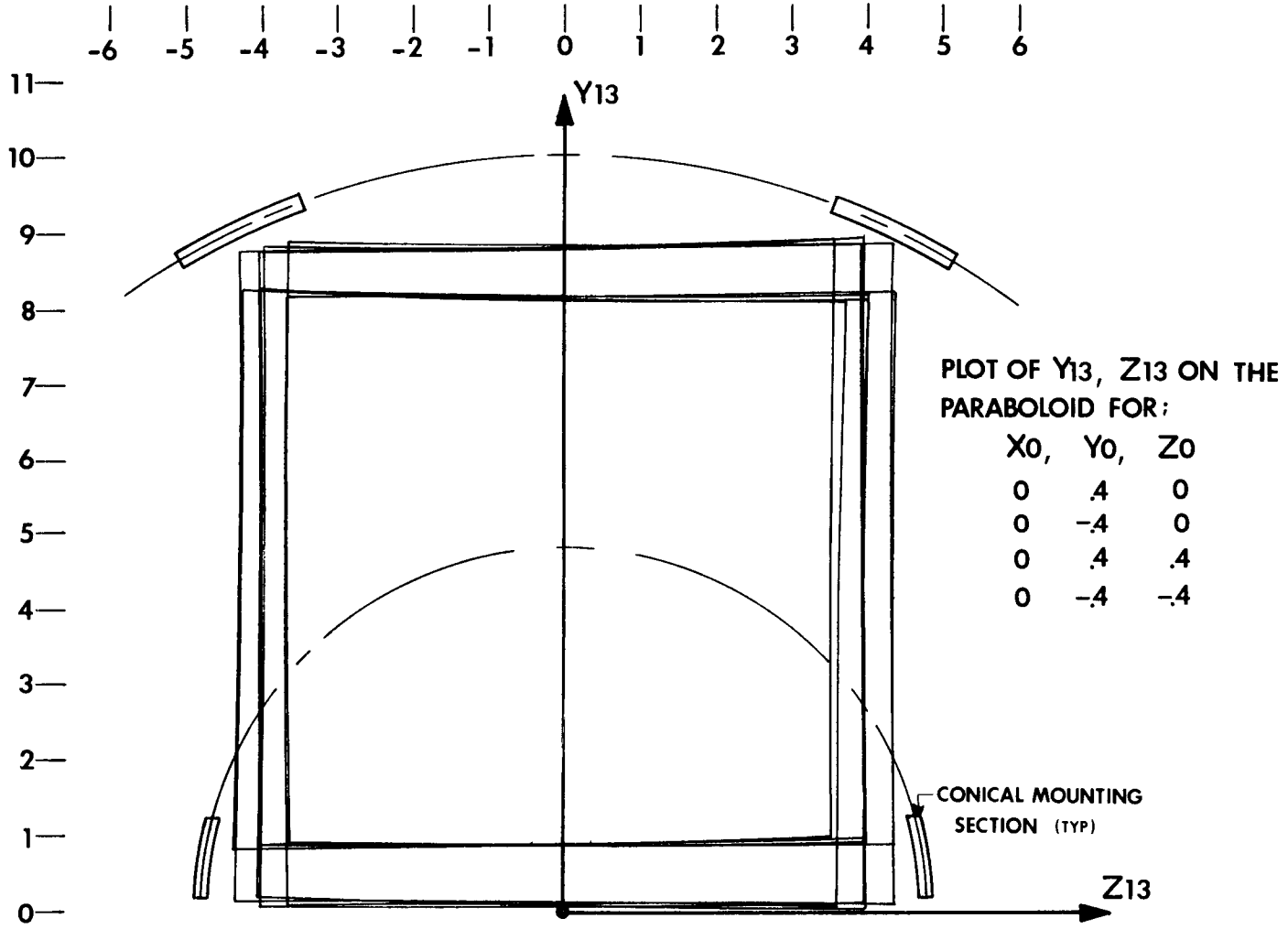

PLOT OF Y_{13}, Z_{13} ON THE PARABOLOID FOR:

X_0,	Y_0,	Z_0
0	.4	0
0	-.4	0
0	.4	.4
0	-.4	-.4

THE AREAS OF USE ON THE PARABOLOID MIRROR SURFACE WHEN THE MIRROR IS BOTH THE 1ST AND 3RD SURFACE. THE 4 SLIT BOUNDRY CONDITIONS ARE USED.

FIG. 9

inches. This will manifest itself as a small wavelength error, and will be substantially corrected by final wavelength calibration procedures.

2.1.10.2 Collimating Mirror

If paraboloid surface of the collimating mirror is used for direct mounting to the monochromator structure as discussed in the previous section, then only this one surface requires tolerances. These surface tolerances should include both general surface irregularities and deviations from a true paraboloid surface, and the accuracy of the focal length.

It has been shown in the previous section that the machined mounting surfaces for this paraboloid mirror should be at their ideal positions within .001 inches. These close tolerances mean that the focusing error contributed by machining these surfaces cannot be greater than .002 inches. It had been assumed that the final slit system positioning methods will correct for defocusing errors up to .040 inches. The remaining .038 inches is then the allowable error in the focal length of the paraboloid mirror.

It is readily seen then that if it were economically feasible to make the paraboloid mirror with a focal length accuracy of ±.001 inches, then the final visual slit alignment techniques would not be required at all. Instead the slits could be positioned mechanically and directly to ±.002 inches of their ideal X04 position as defined by the ray trace. Thus the complete monochromator optical system would be free of adjustments, which is a real aid to obtaining high reliability and repeatability of performance.

The decision as to whether to build the monochromator without adjustment which will also make the slit mountings much simpler, or whether to provide facilities for later visual alignment and fixing of the slit location will depend on the feasibility of obtaining the paraboloid with a 20.000 ±.001 inch focal length.

Irregularities in the surface of the paraboloid will cause rays from these irregular areas to deviate from their ideal position on the exit slits. For this monochromator with a 20 inch focal length, irregularities equivalent to two fringes/inch will cause exit slit error deviations of .001 inches. However, since in practice the paraboloid mirror may not be tested by interferometry during its construction, a better definition of surface accuracy may be to require that the mirror will focus a perfectly collimated beam of light which covers the area of use on the paraboloid into a circle of confusion no larger than .002 inches in diameter at the focal plane.

2.1.10.3 Grating

The grating is mounted in the (X2, Y2, Z2) axis system. The accuracy to which it is mounted in this axis system will now be discussed. In the first place, the error in locating the grating along the X2 axis has negligible effect on the image at the exit slit. However, the magnitude of this error may be critical when considered relative to the position of the wavelength cam axis. The spacing between the cam axis and grating axis must be held to quite high accuracy if wavelength accuracy is to be of a high order. The effect of such an error must be computed from the combined cam-cam follower geometry, but usually these axes need an accuracy of spacing of $\pm$ .0005 inches, and often times, much less.

The Y2 axis should be parallel to the lines of the grating. If instead the lines are tilted forward or backward in the X2 - Y2 plane, then the exit slit image will be low or high, respectively, in relation to the exit slit position. At high incident grating angles, however, some lateral tipping of the exit slit image will also occur which will act as both a wavelength error and a wavelength bandwidth broadening factor. The grating lines should be oriented within $\pm$ 1 minute of arc of the Y2 axis as measured in the X2 - Y2 plane. This will keep the magnitude of the Z04 error within .001 inches.

If the lines of the grating are tilted in the Y2 - Z2 axis, a stronger exit slit image tilt will be observed. This will manifest itself in a Z04 image displacement which will be both a direct wavelength error and a wavelength bandwidth broadening factor. The grating lines should be oriented within $\pm$ .5 minutes of arc of the Y2 axis as measured in the Y2 - Z2 plane. This will keep the magnitude of the Z04 error within .001 inches.

The actual process of mounting a grating on its bearing axis to these tolerances may be done by two general approaches. The first is to align the grating by purely mechanical means in a precision jig borer or similar accurate tool. Surfaces are indicated using mechanical or electronic indicators. The position of the lines may be located and positioned by a microscope.

The second method consists of mounting the grating bearing axis perfectly normal to an autocollimator. Next the grating face is made also normal to the autocollimator. Then the lines of the grating must be brought into parallelism with the bearing axis by obtaining simultaneous autocollimation

for the grating at the zero order and all other orders, positive or negative, which are visible. A low pressure mercury source with line spectra is required for the autocollimator.

2.1.10.4 Slits

The exit slit must be located as accurately as possible on the entrance slits image at the exit slit plane. The ray trace has carefully determined the locations of the neutral axes of the entrance and exit slits and has determined the required curvature of the entrance slit. The slit jaws should now be located as accurately as possible to reproduce these ideal conditions. The defining jaws of the two slits should have actual Y04 and Z04 locations within $\pm$ .0003 inches of each other. All of the defining jaws must also lie in the same plane. This relative positioning accuracy is usually accomplished by use of a precision assembly jig which must be designed and constructed for this one purpose.

The slit jaws should be completely supported during operation by a spring hinge system. There must be no mechanical friction involved in the slit operation, otherwise erratic energy output from the monochromator may be observed. A complete spring hinge system will be trouble free for vacuum operation and over the wide temperature range required of the monochromator..

2.1.10.5 Effects of Temperature and Vacuum

The performance of the calibration monochromator would be substantially degraded by operation in vacuum and at very low ambient temperatures unless proper precautions are taken in the mechanical design. Some of the main problems to be considered when operation is in a vacuum are the following:

1. Journal bearings and sliding bearing can seize and become inoperative.
2. Improper surface processing of castings can cause excessive out-gassing and increased time required for pump-down.
3. Certain lubricants may out-gas severely and be deposited on optical elements and then reduce transmission of the system.
4. Plastic coatings, such as the replicated grating surface, may be damaged if improperly applied.

All of the above innumerated problems can be avoided by good vacuum engineering practices.

To maintain performance within specifications for the calibration monochromator over the wide operating temperature range from $80^{o}K$ to $300^{o}K$ requires solving two types of problems. The first type of problem is very similar to the problems created by vacuum.

1. Journal bearings and sliding bearings lock and become inoperative due to differential expansion of various bearing components.
2. There are very few desirable lubricants for this wide range of temperature.
3. The replica coating on the grating may check if improperly made because of differential expansion between the coating and the support.

Similar to the case of vacuum operation, these above problems can be solved by good cryogenic engineering practices.

The second type of problem, caused by the large temperature range requirements of the monochromator, is that of dimensional changes to all monochromator parts, and the resultant degradation of performance below specifications. The following discussion presents only a generalized approach to this problem. The detail solutions must be considered in light of the actual mechanical layout. First, let us assume we have designed a complete monochromator of monometalic construction. This means that the main structure, mirror, grating, cam, slits, and all other aiding parts and components are made from the same material, which may be aluminum, glass, etc. Let us ask then what type of performance this monochromator will have at ambient temperatures of both $80^{o}K$ and $300^{o}K$. It will be found then that this monochromator will retain the same sharp focus at any stable and uniform temperature, but it will not retain the same wavelength calibration.

When the temperature is lowered $220^{o}C$ in going from $300^{o}C$ to $80^{o}C$, there will be a shrinkage in the size of all parts. However, for monometalic construction all parts have the same percent shrinkage. The monochromator can then retain constant focus because the monochromator distance from the slit to the collimating mirror is shortened by the same percentage as is the focal length of the paraboloid mirror.

To define the effect on the wavelength calibration of the monochromator caused by a large drop in temperature let us refer to the grating equation for a littrow monochromator which is equation (2).

$$N\lambda = 2a \sin i$$

The sin i function is actually controlled by the ratio of the effective radius of the cam to the length of the wavelength arm. However, in the monometalic system, this proportion remains constant and thus so does sin i. It can then be seen by equation (2) that, if sin i is constant, then λ will be a linear function of the grating line spacing, a. However, the grating line spacing, a, will not be constant since this has the same shrinkage rate as the grating replica support. It is seen from equation (2) then, that the wavelength λ will be shifted to a shorter wavelength by reducing the temperature. This latter wavelength shift can be greatly reduced in this monometalic monochromator by laying the grating replica on fused silica or Pyrex glass which have very small coefficients of expansion.

The next question to answer then is how practical it is to accomplish monometalic construction. In the first place, a stabilized aluminum casting is probably the best material for the monochromator structure. Aluminum castings are economical, lightweight, very castable and machinable, and they can be aged for high stability. They also have high thermoconductivity which allows their rapid stabilization to uniform temperature after a temperature change. This latter property often makes aluminum considerably more desirable then steel, which requires considerably more time for temperature stabilization. Also, steel can retain larger undesirable temperature gradients due to different temperatures on opposite sides of the part.

The paraboloid collimating mirror can be made of aluminum. Aluminum mirrors have been made by using a thin hard surface coating, then final polishing and aluminizing it. Such a mirror would maintain a sharp focus for the monochromator at all temperatures. If the collimating mirror is made of glass, it should be one with a high coefficient of thermal expansion such as crown glass.

An aluminum casting alloy of high silicon content, such as A132, has a coefficient of thermal expansion of 19.0×10^{6} inches/high/^{o}C, whereas, some crown glasses have a coefficient of thermal expansion as high as 11.3×10^{-6} inches/inch/^{o}C. These latter coefficients are for a temperature of 300^{o}C and will be different at 80^{o}K. By using the coefficients at 300^{o}C, it is seen that aluminum A132 has a greater coefficient of expansion than crown glass by 7.7×10^{-6} inches/inch/^{o}C. The magnitude of defocus measured along the X04 axis for a temperature change from 300^{o}C to 80^{o}C is

$$7.7 \times 10^{-6} \times 20 \times 220 = .035 \text{ inches}$$

Then, as was described in Section 2.1.10, an X04 error of .035 inches will cause a Z04 image spread of .014 inches. This image spread is slightly greater than .3 mm. The designer must decide between an aluminum or glass mirror. The aluminum mirror is more expensive at this time.

Now going to the wavelength calibration change problem, we are immediately confronted with the difficulty of obtaining a good aluminum cam. This is possible, but at greater cost than an all-steel cam. The aluminum cam would require the final cam surface to be hard coated for wear. The other approach

is to use a steel cam, a steel wavelength arm on the grating, and a steel spacer between the grating bearing system and the cam bearing system; thus, the constancy of the sin i function will once again be preserved. Other more complex approaches are possible, such as using different metals for the cam and the wavelength arm with the planned purpose of compensating for changes in grating line spacing, a, due to the expansion of the replica grating support.

2.2 Optical Coupling for the Calibration Monochromator

The calibration monochromator is to be used to illuminate other monochromators undergoing performance tests. It is of prime importance that the calibration monochromator be capable of filling completely and uniformally both the entrance slit and the aperture of the dispersive element of the test monochromator. The monochromator which was described in the Final Report, Phase II, prepared under Contract 950880 for Jet Propulsion Laboratory by Beckman Instruments, Inc., presents difficult and typical optical coupling problems which can only be adequately solved by ray-trace techniques. This particular test monochromator is used for illustration, since a complete set of boundary rays are already programmed.

Two different optical coupling systems have been analyzed for use between the calibration and test monochromators. In one system a single spherical concave mirror is used to image the exit slit of the calibration monochromator onto the entrance slit of the test monochromator without using the spherical entrance telescope mirror of the test monochromator. In the other system the test monochromator retains its spherical entrance telescope mirror and the calibration monochromator is also provided with an identical spherical telescope mirror for collimating light between the two telescope mirrors. In

this latter system, the exit slit of the calibration monochromator is again imaged onto the entrance slit of the test monochromator.

For both the single mirror and the double mirror coupling systems it was found advantageous to use the computer ray trace with those same rays which were used in the Contract 950880 report, which fill the slit aperture of the test monochromator. These rays have been used in their reverse direction and traced, in order, through the coupling optics, through the exit slit plane of the calibration monochromator, and onto the grating aperture of the calibration monochromator. The orientation of the calibration monochromator relative to the coupling optics had to be modified and retraced many times until (1) the entrance slit image of the test monochromator was accurately imaged on the exit slit of the calibration monochromator; and (2) the test monochromator aperture was imaged within the bounds of the grating aperture of the calibration monochromator. The details of this positioning will now be discussed.

2.2.1 Single Mirror Coupling Optics

In Figure 10 are shown the locations of the calibration and test monochromators and the single coupling mirror. The (XO, YO, ZO) axis system is the entrance slit location for the test monochromator. The remainder of this monochromator is not shown, but the defining rays for this monochromator are used.

The rays commence in the (XO, YO, ZO) axis system, and the directional cosines of these rays are first multiplied by (-1) so the rays are given an opposite

FIG.10

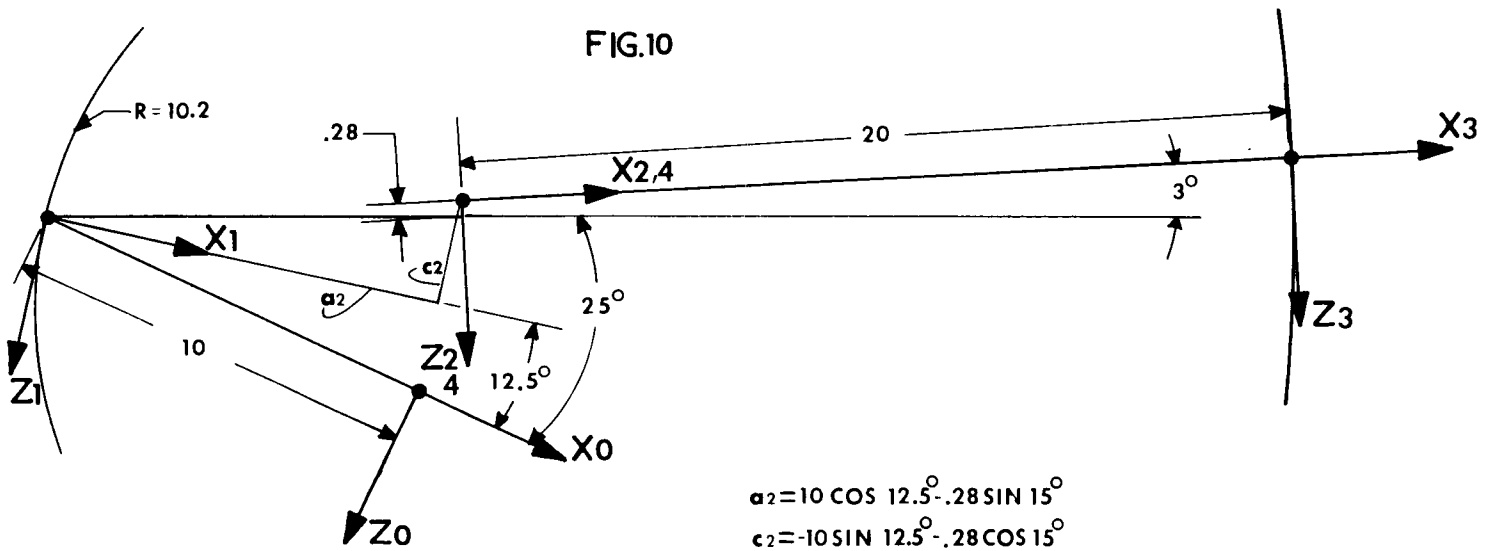

$a_2 = 10 \cos 12.5^\circ - .28 \sin 15^\circ$

$c_2 = -10 \sin 12.5^\circ - .28 \cos 15^\circ$

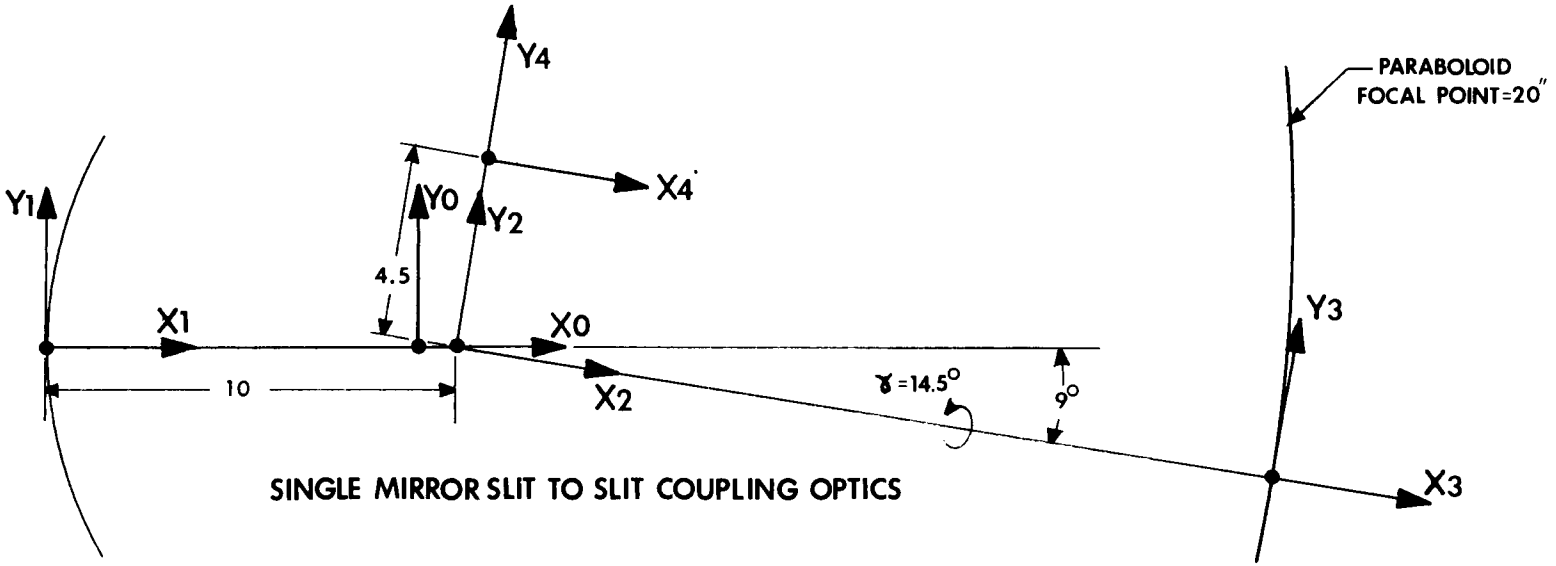

SINGLE MIRROR SLIT TO SLIT COUPLING OPTICS

direction or sense. These rays are then directed toward the spherical coupling mirror. The spherical coupling mirror is in the (X1, Y1, Z1) axis system. The exit slit of the calibration monochromator is in the (X2, Y2, Z2) axis system. The origin of the (X2, Y2, Z2) axis system is offset .28 inches along the -Z04 axis which is the exit slit neutral axis offset. The calibration monochromator collimating mirror is in the (X3, Y3, Z3) axis system and the grating is in the (X4, Y4, Z4) axis system.

It will be observed that the calibration monochromator has acquired a substantial twist relative to the incoming beam from the coupling mirror. This is necessary because of the severely tilted slit of the test monochromator. The (X2, Y2, Z2) axis system rotational position relative to the (X1, Y1, Z1) axis system is:

$$\alpha\ 2 = -15.5^{\circ}$$
$$\beta\ 2 = -\ 9^{\circ}$$
$$\gamma\ 2 = \ 14.5^{\circ}$$

Figure 10 completely defines the coupling optics and relative location of the two monochromators.

2.2.2 Double Mirror Coupling Optics

This system is shown in Figures 11a and 11b. Again, the entrance slit of the test monochromator is in the (X0, Y0, Z0) axis system. The telescope mirror of the test monochromator is in the (X1, Y1, Z1) axis system. An identical telescope mirror is mounted in the (X2, Y2, Z2) axis system. The exit slit of the calibration monochromator is now in the (X3, Y3, Z3) axis

FIG. 11A

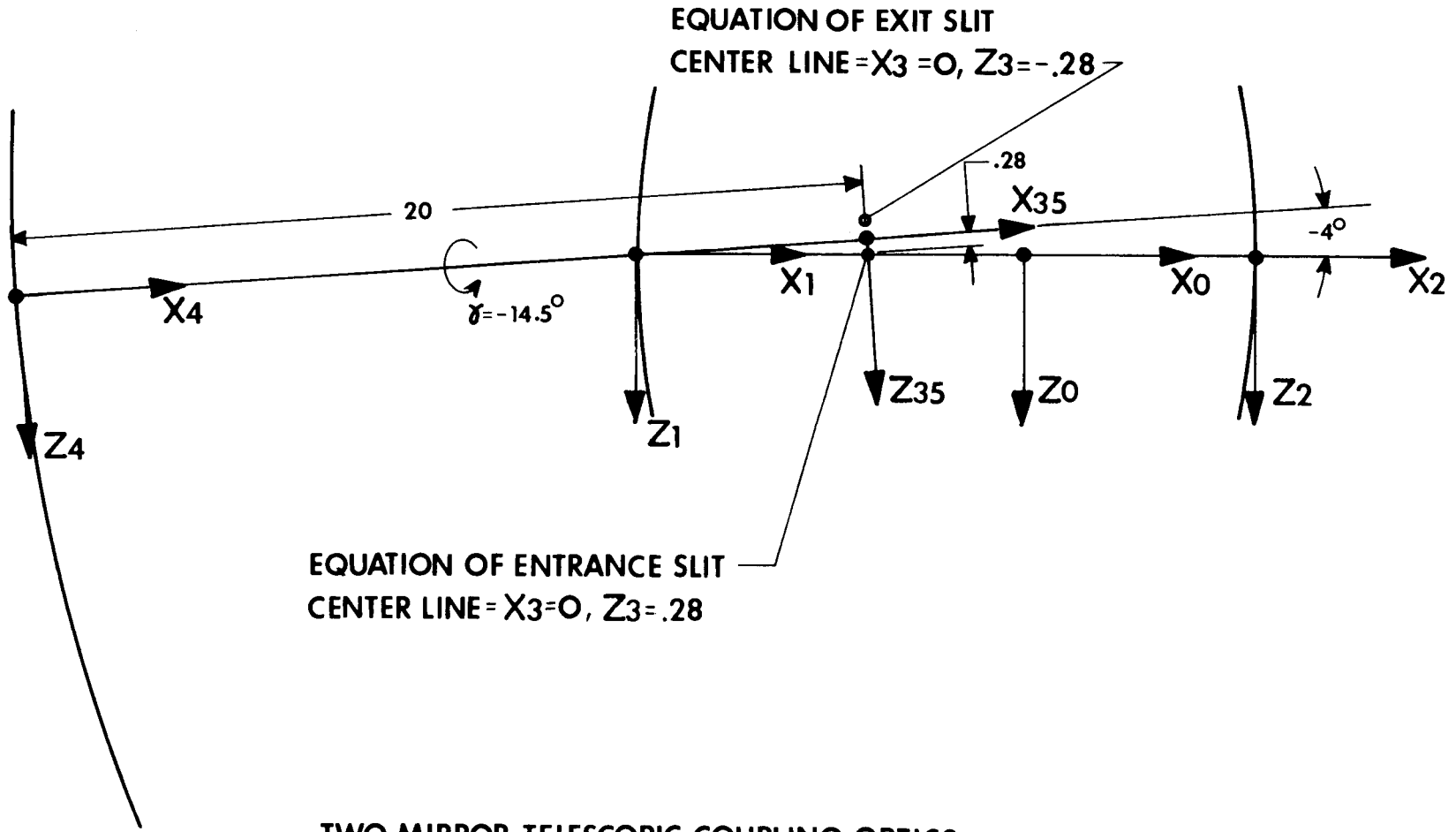

TWO MIRROR TELESCOPIC COUPLING OPTICS

(X - Z VIEW)

FIG. 11B

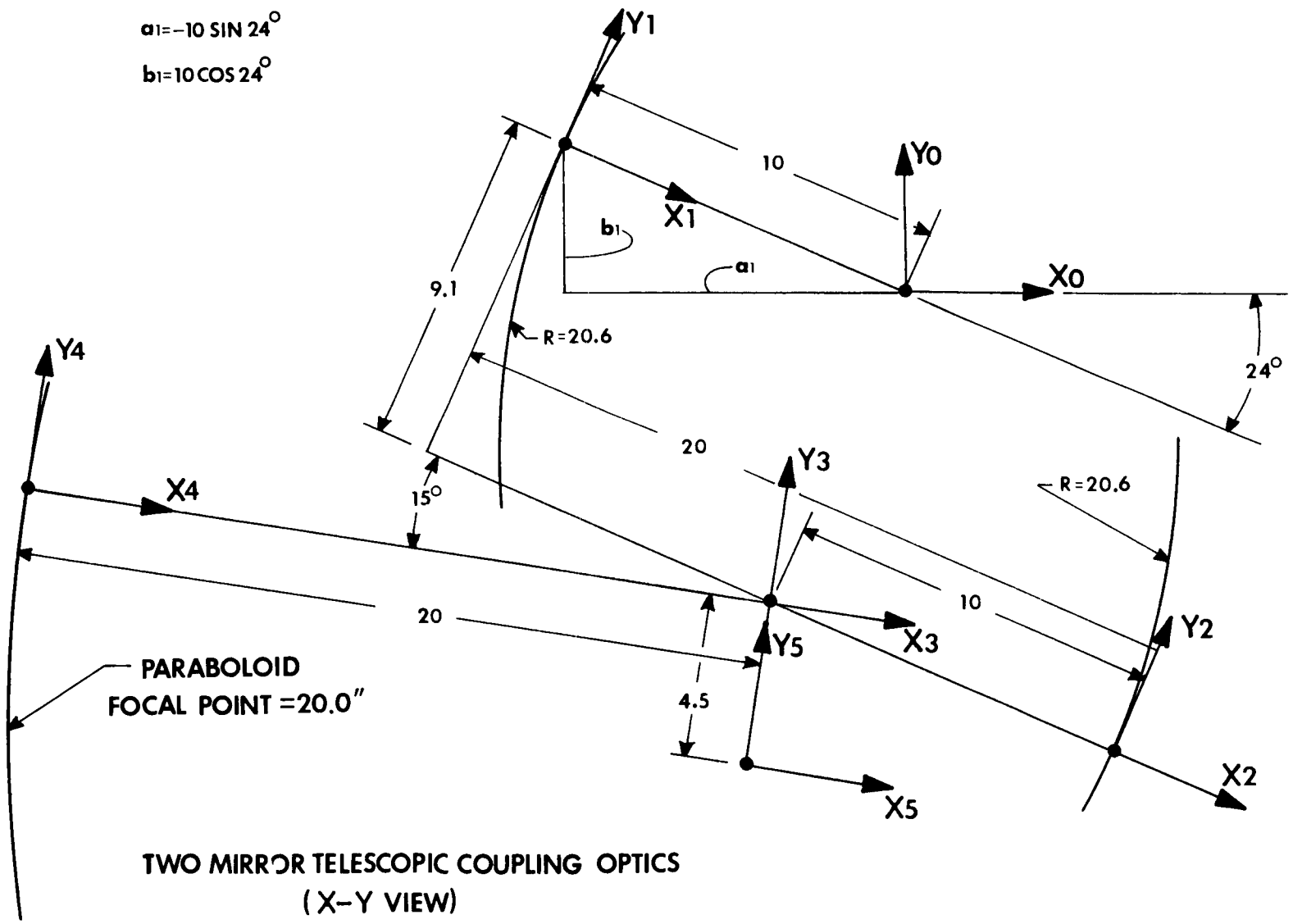

TWO MIRROR TELESCOPIC COUPLING OPTICS
(X-Y VIEW)

system; the collimating mirror of the calibration monochromator is in the (X4, Y4, Z4) axis system, and the grating of the calibration monochromator is in the (X5, Y5, Z5) axis system. Again, it is seen that the calibration monochromator requires a substantial twist relative to the test monochromator, and here also the calibration monochromator has been turned upside down in order to obtain best coupling efficiency. It may be an important factor in the design of the calibration monochromator to have it operate in any orientation. Figures 11a and 11b completely define the coupling optics and the locations of the monochromators.

2.2.3 Results of Ray Trace

Figure 12 shows images of the grating aperture of the test monochromator at the grating aperture of the calibration monochromator. The different images represent different ray starting points on the entrance slit of the test monochromator. These points define the boundaries of the 3 mm x 15 mm entrance slit, and the center of the slit. The test monochromator has an f/3.5 square aperture and the calibration monochromator has an f/2.5 square aperture, thus the image of the test monochromator aperture is seen to be much smaller than the aperture of the calibration monochromator.

Figure 13 is the same type of image presentation as Figure 12, except it is for the two-mirror system. The two-mirror system has produced a near-perfect image of the test monochromator aperture on the calibration monochromator aperture which results in the near superposition of the images for all five ray starting points at the entrance slit of the test monochromator. Figure 12, on the other hand, shows that the test monochromator aperture is well out

ZONES OF ILLUMINATION ON THE CALIBRATION MONOCHROMATOR APERTURE FOR RAYS FROM FIVE POINTS ON THE TEST MONOCHROMATOR SLIT. CASE FOR SINGLE MIRROR COUPLING OPTICS.

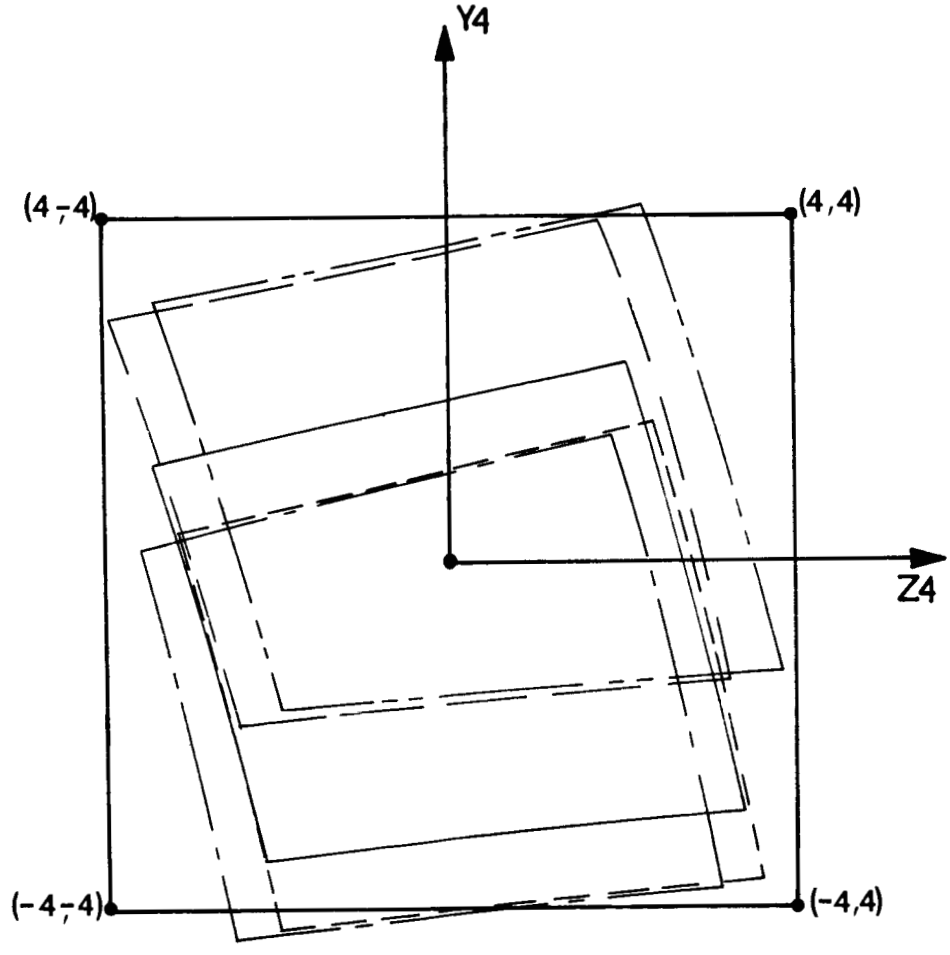

Xo	Yo	Zo	
0,	0,	0	———————
.05,	.20,	-.01	— — — —
.05,	.20,	.11	—— - ——
.12,	-.40,	-.16	—— - - ——
.12,	-.40,	-.04	—— —— ——

FIG. 12

ZONES OF ILLUMINATION ON THE CALIBRATION MONOCHROMATOR APERTURE FOR RAYS FROM FIVE POINTS ON THE TEST MONOCHROMATOR SLIT. CASE FOR TWO MIRROR TELESCOPIC COUPLING OPTICS.

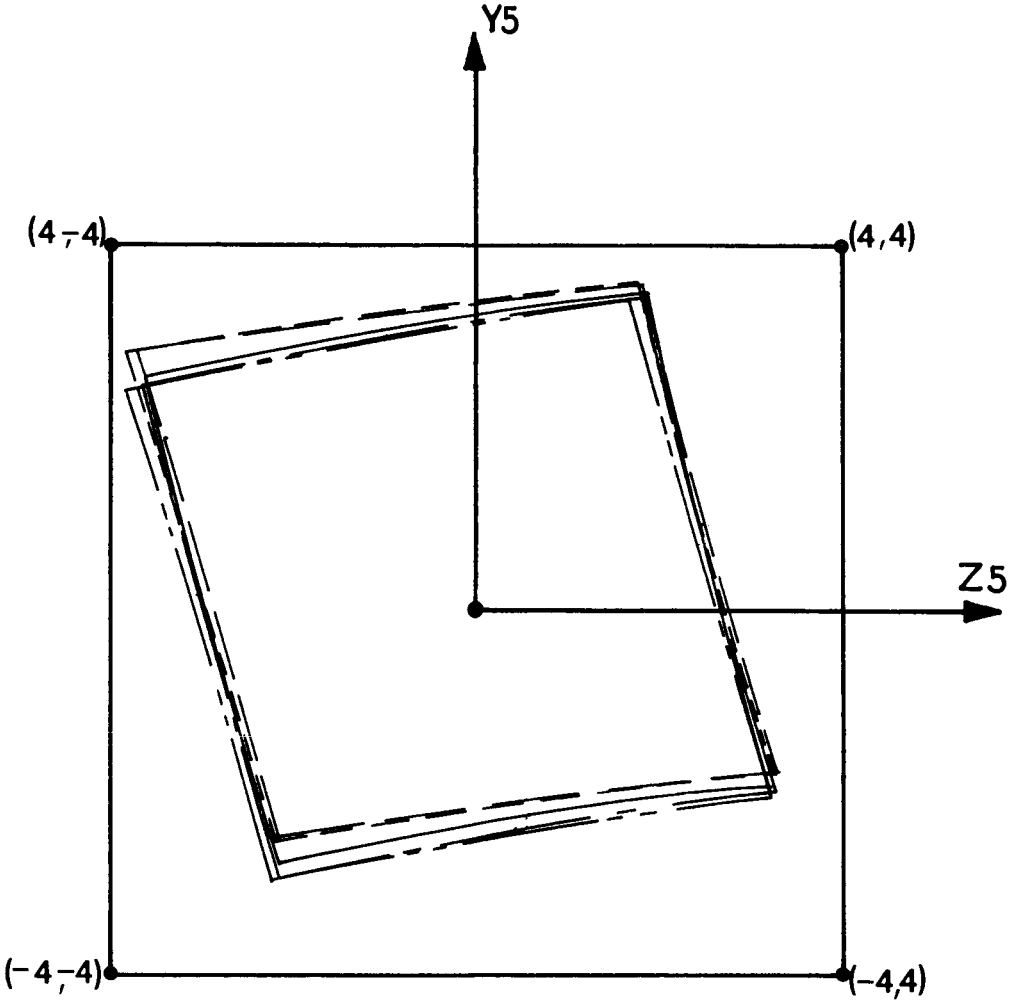

Xo	Yo	Zo	
0,	0,	0	———
.05,	.20,	-.01	——·———
.05,	.20,	.11	—— -- ——
.12,	-.40,	-.16	—— —— ——
.12,	-.40,	-.04	— — — — —

FIG.13

of focus at the calibration monochromator aperture when the single coupling mirror is used. This, of course, affects nothing more than the image spread on the calibration monochromator aperture. Figures 14 and 15 show, respectively, the images formed at the exit slit plane of the calibration monochromator for the single mirror optical coupling system, and for the double mirror optical coupling system. The X2 and Z2 axes of the calibration monochromator are the slit axes used in Figure 14 and the X3 and Z3 axes are the slit axes used in Figure 15. Both figures use the same three ray starting points in the (X0, Y0, Z0) axis system, which is the slit axis of the test monochromator.

Each of the three graphs of Figures 14 and 15 show the maximum Z2 or Z3 spread of rays from a single ray starting point on the slit of the test monochromator. They show that the single mirror coupling system can give a slightly better image at the calibration monochromator exit slit than the two-mirror coupling system. It is also seen that the image on the exit slit of the calibration monochromator for a single point on the test monochromator slits may have a Z component as large as .16 inches or 4 mm. Thus, if the calibration monochromator is to pass every ray required by the test monochromator which has slit widths of 3 mm, then it is required that the slit width of the calibration monochromator be 7 mm.

Figures 14 and 15 also show, respectively, the focusing effects for different slit positions along the X2 and X3 axes. These focusing ranges may be as great as .1 inches with only a small percentage change in the Z2 and Z3 error.

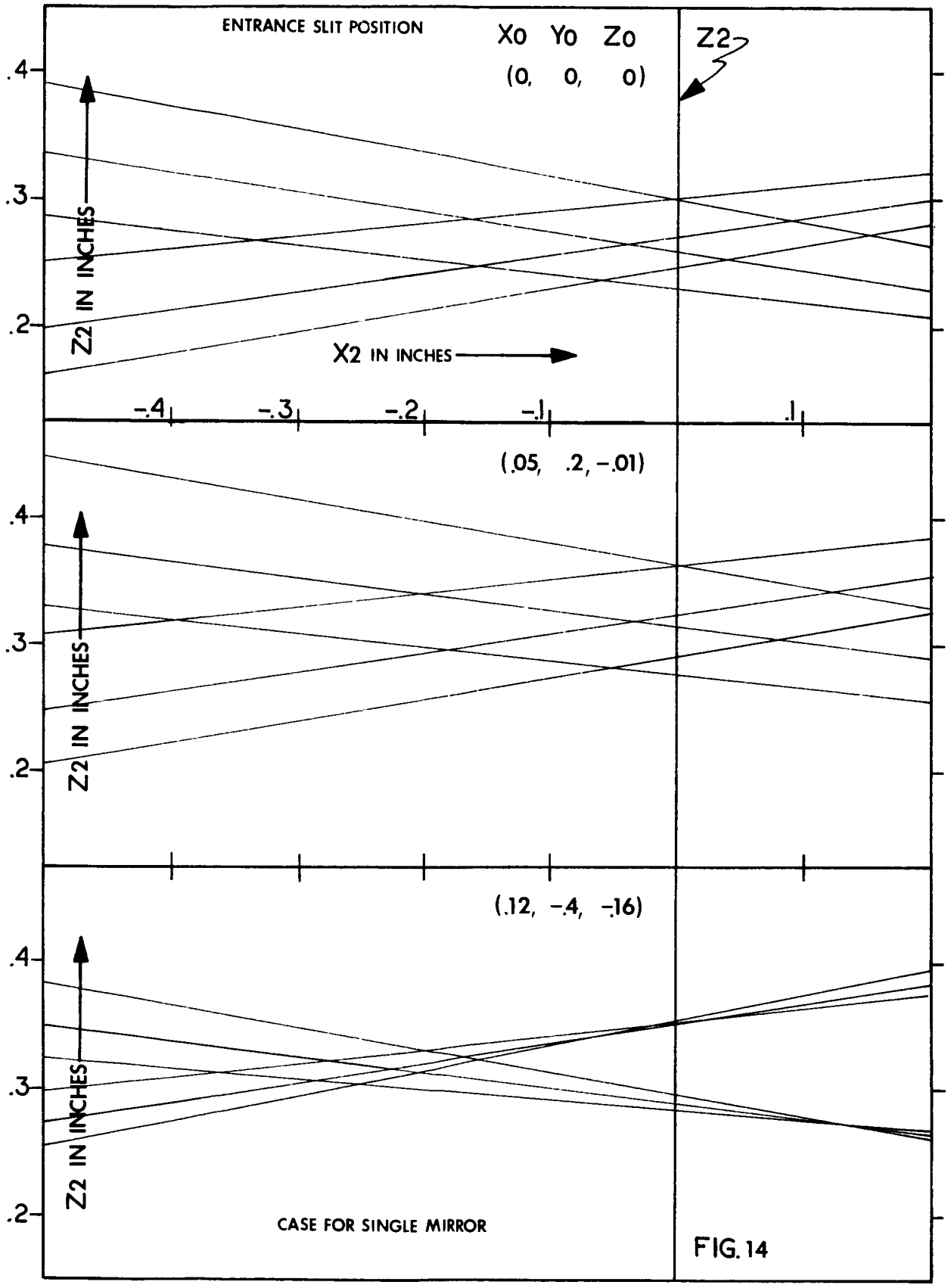
ENTRANCE SLIT POSITION
X0 Y0 Z0
(0, 0, 0)
Z2
.4
.3
.2
Z2 IN INCHES
X2 IN INCHES
-.4
-.3
-.2
-.1
.1
(.05, .2, -.01)
(.12, -.4, -.16)
CASE FOR SINGLE MIRROR

FIG. 14

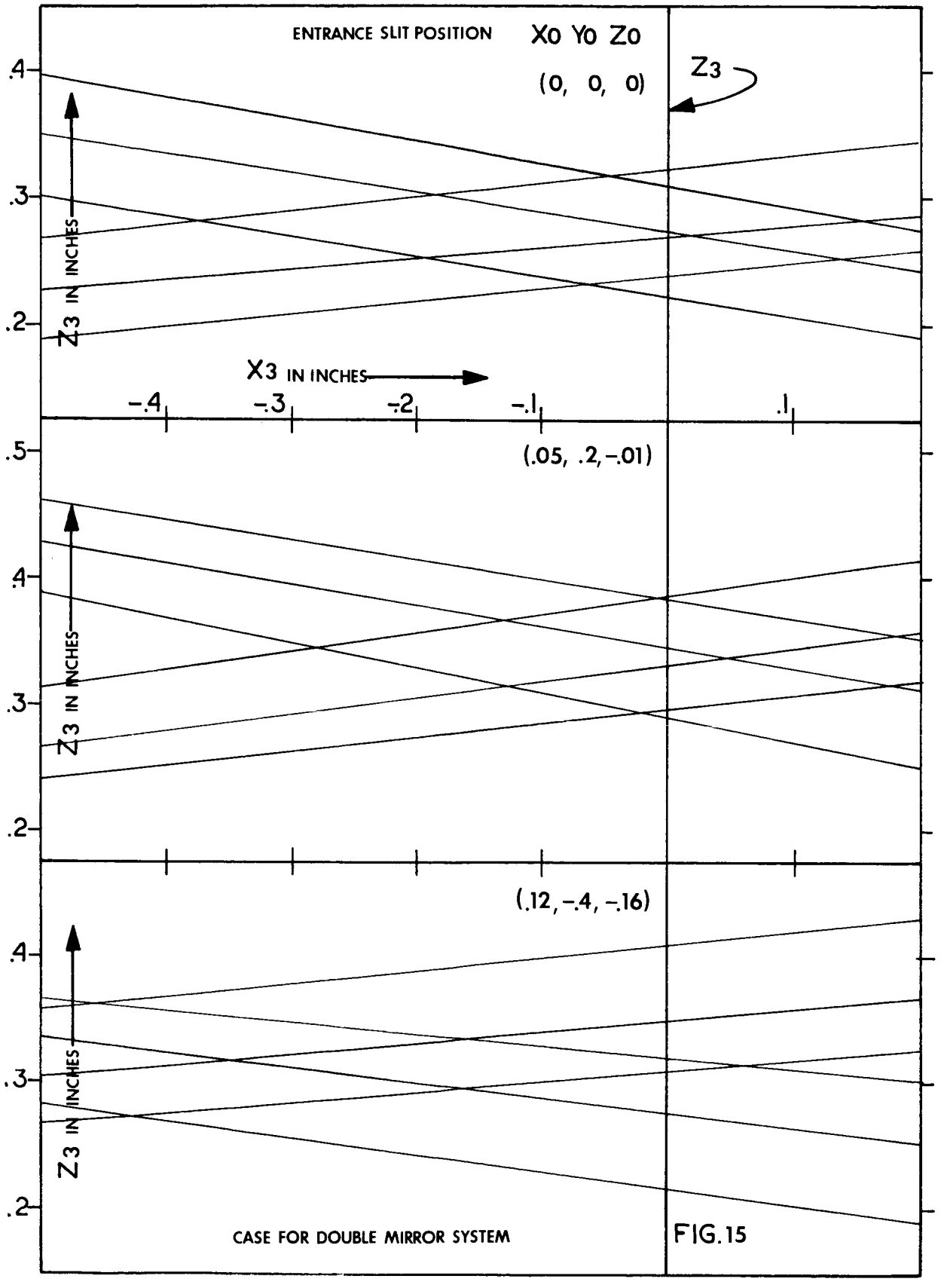
ENTRANCE SLIT POSITION
Xo Yo Zo
(0, 0, 0)
Z3
.4
.3
.2
Z3 IN INCHES
X3 IN INCHES
-.4
-.3
-.2
-.1
.1
.5
(.05, .2, -.01)
.4
.3
.2
Z3 IN INCHES
(.12, -.4, -.16)
.4
.3
.2
Z3 IN INCHES
CASE FOR DOUBLE MIRROR SYSTEM

FIG. 15

2.3 Approximate Dimensions of Optical Components

2.3.1 Gratings:

Ruled Areas - 200 mm high x 315 mm wide

Blaze Angle - 25^{o}

Lines/mm - 100, 250, 600

2.3.2 Collimating Mirror:

To be cut from paraboloid mirror with following dimensions:

Usable Diameter	20.2 inches
Focal Length	20.000 $\pm$ .038 inches
(Alternate focal length for complete monochromator without adjustment)	20.000 $\pm$ .001 inches
Surface Accuracy	Image circle of confusion for axial parallel illumination is .002 inches diameter

This mirror may be cut precisely in half and each half further shaped to make collimating mirrors for two monochromators.

A P P E N D I X

Some pertinent information regarding this project, and which may prove useful in the study of the design features discussed in the Final Report, was included in the Beckman Technical Proposal. The pertinent portions of this Proposal are included as an Appendix to this Report.

2.0 TECHNICAL DISCUSSION

2.1 General

The design of a monochromator having the performance characteristics required for the specified calibration purposes presents several unusual and difficult problems. Among the factors which must be considered, in order to attain the optimum optical system, are the high degree of resolution necessary, the stray energy characteristics of the system, and the environmental conditions under which the monochromator will be operated. These factors will, for the most part, dictate certain desirable or necessary design details, from which the overall monochromator design will be developed. Each of these factors is considered separately in the following paragraphs, followed by a summary of the considerations which will enter into the development of the final design.

2.2 Resolution

The very high resolution requirements for the calibration monochromator demand that gratings be used. There are two general systems for using gratings: System (1) uses a fixed entrance slit, a fixed grating position, and a movable exit slit or multiple exit slits or film. System (2) has both entrance and exit slits fixed, and a rotatable grating.

System (1) used at f/3 suffers from a very large change in the magnitude of optical aberrations across the exit slit image plane. This has been shown in "Study and Investigation of Optical System", Phase I, Final Report, Con-

tract 950880, Prepared by Beckman Instruments, Inc. for JPL. It was shown that for one ideal position on the exit slit image plane that aberration can be held to .2 mm. However, the exit slit image aberration will be 6 times larger at wavelengths displaced 18° to either side. System (2) allows the exit slit to maintain its ideal location for all wavelengths. Only the grating is rotated for scanning wavelengths. The angular position of the grating modifies the aberration pattern at the exit slit only slightly. Thus an f/3 monochromator of high resolution demands system (2).

The resolution and resolving power of a grating monochromator may be found as follows:

The general grating equation is

$$N\lambda = a\ (\sin i + \sin\theta)$$

where

N = grating order

λ = wavelength of light in μ

a = grating line spacing in μ

i = incident angle of light on grating

θ = diffracted angle of light from grating

For system (1) angle i is constant for all wavelengths while angle θ varies. For system (2) both angle i and angle θ vary together and for wavelength determinations of the monochromator they may be considered equal. For resolution determinations they are also taken to be nearly equal but with angle i kept constant at a given wavelength and angle θ allowed to vary about it.

Differentiating the general equation

$$Nd\lambda = a \cos\theta\ d\theta$$

and $\frac{d\theta}{d\lambda} = \frac{N}{a \cos \theta}$ (radians/μ)

This is the angular dispersion function.

The linear dispersion at the exit slit is then

$$\frac{ds}{d\lambda} = \frac{Fd}{d\lambda} = \frac{FN}{a \cos \theta} \quad (mm/\mu)$$

where

F = focal length of monochromator in mm

ds = spectral spread at exit slit in mm

The value (ds) may also be considered the exit slit width when finding the monochromator resolution for a given slit width. Then the monochromator resolution is:

$$d\lambda = \frac{a \cos \theta \, ds}{FN} \quad (\mu)$$

If we introduce the term, k, which designates the number of lines/mm of the grating then the resolution equation becomes

$$d\lambda = \frac{1000 \cos \theta \, ds}{k \, FN} \quad (\mu)$$

The resolving power of a monochromator is defined as

$$R = \frac{\lambda}{d\lambda}$$

and substituting for λ and $d\lambda$

$$R = \frac{a/N \, (\sin i + \sin \theta)}{(a/FN) \cos \theta \quad ds}$$

and finally:

$$R = \frac{F(\sin i + \sin \theta)}{ds \quad \cos \theta}$$

This last equation is a general equation for the resolving power of a grating monochromator with a given slit width (ds), when (ds) is larger than the resultant half bandwidth due to the combined diffraction and optical aberrations at the exit slit.

For the littrow type monochromator where angles i and θ are nearly equal, resolving

power may be written as approximately

$$R_L = \frac{2F \sin i}{ds \cos i}$$

and

$$R_L = \frac{2F \tan i}{ds}$$

The grating presents many problems when the wavelength range to be covered is large such as the wavelength range fron 1μ to 15μ required for the calibration monochromator. This is a wavelength magnitude change of 15x. Any grating operated in its first order has an energy efficiency more than 50% for only a range of 2.5x. In the second order the 50% efficiency range is reduced to 1.55x. Graphs I, II, III, and IV show four different grating plans. All gratings used for the first three graphs are standard B & L gratings in the 84 x 84 mm size. Definite improvements are possible by using non-standard gratings. On each graph are shown by solid lines the theoretical efficiency of the gratings normalizing the efficiency to 1.0 at the blaze wavelength. (Real gratings have actual efficiences at the blaze wavelength as high as .85).

The graphs show the incident angle i or diffracted angle (assuming here they are equal) as dashed lines. The half bandwidth resolution $d\lambda$ for an exit slit of .3 mm and a monochromator focal length of 10 inches is shown as the dash-dot lines. The resolving power $\frac{\lambda}{d\lambda}$ is shown as the dotted lines.

Graph I shows an arrangement using three separate gratings each in its first order. They are respectively a 300 1/mm, 150 1/mm and 75 1/mm grating. The 300 1/mm grating is used from 1μ to 2.6μ. The 150 1/mm grating is used from 2.6μ to 6μ. The 75 1/mm grating is used from 6μ to 15μ. These gratings must be in a mount which allows them to mechanically replace one another. This arrangement has excellent energy efficiency. Nearly all wavelengths are above an efficiency of .5.

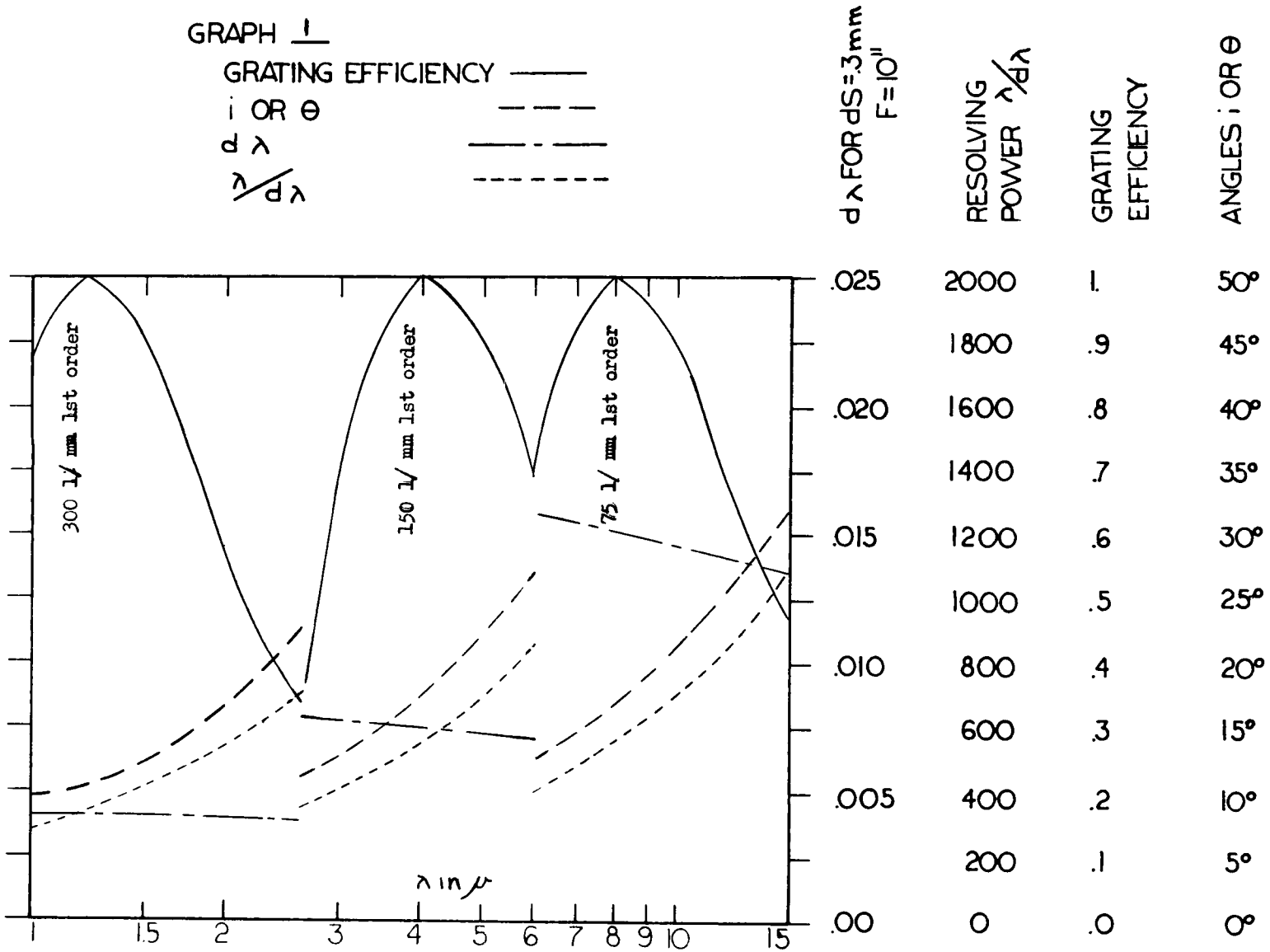
GRAPH 1
GRATING EFFICIENCY
i OR θ
d λ
λ/d λ
300 l/ mm 1st order
150 l/ mm 1st order
75 l/ mm 1st order
λ in μ
1
1.5
2
3
4
5
6
7
8
9
10
15
d λ FOR dS=.3mm F=10"
.025
.020
.015
.010
.005
.00
RESOLVING POWER λ/dλ
2000
1800
1600
1400
1200
1000
800
600
400
200
0
GRATING EFFICIENCY
1.
.9
.8
.7
.6
.5
.4
.3
.2
.1
.0
ANGLES i OR θ
50°
45°
40°
35°
30°
25°
20°
15°
10°
5°
0°

GRAPH II

GRATING EFFICIENCY ——

i OR θ — — —

dλ —·—·—

λ/dλ - - - - -

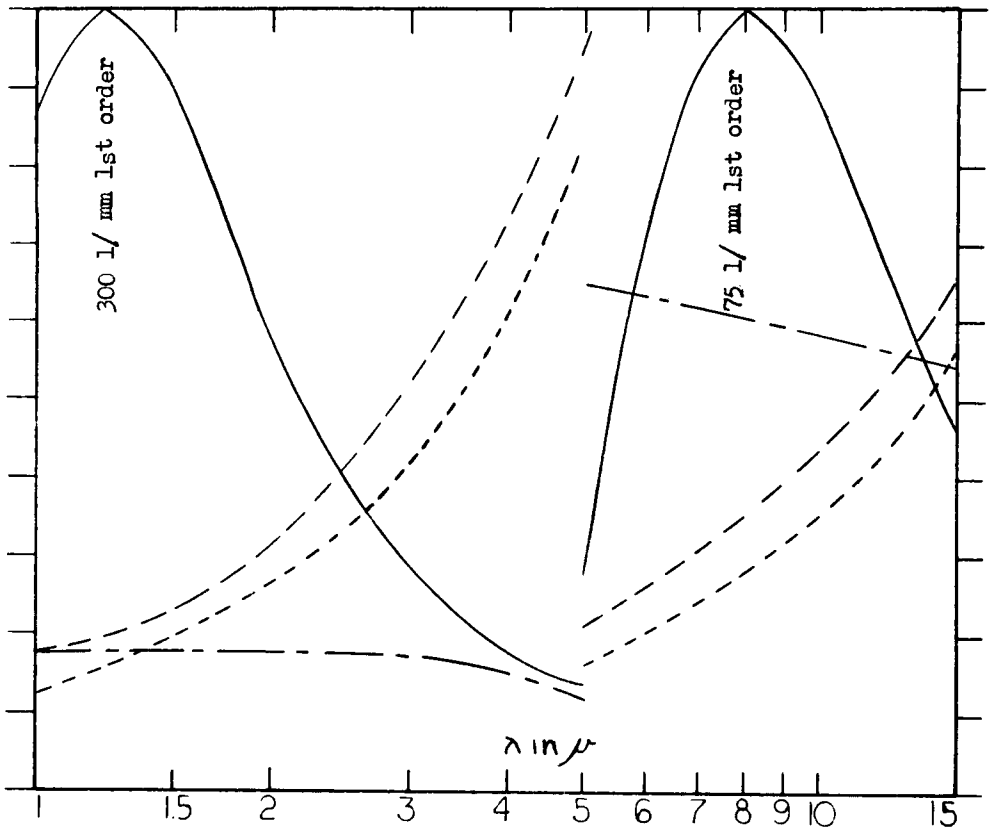

dλ FOR dS=.3mm F=10"	RESOLVING POWER λ/dλ	GRATING EFFICIENCY	ANGLES i OR θ
.025	2000	1.	50°
	1800	.9	45°
.020	1600	.8	40°
	1400	.7	35°
.015	1200	.6	30°
	1000	.5	25°
.010	800	.4	20°
	600	.3	15°
.005	400	.2	10°
	200	.1	5°
.00	0	.0	0°

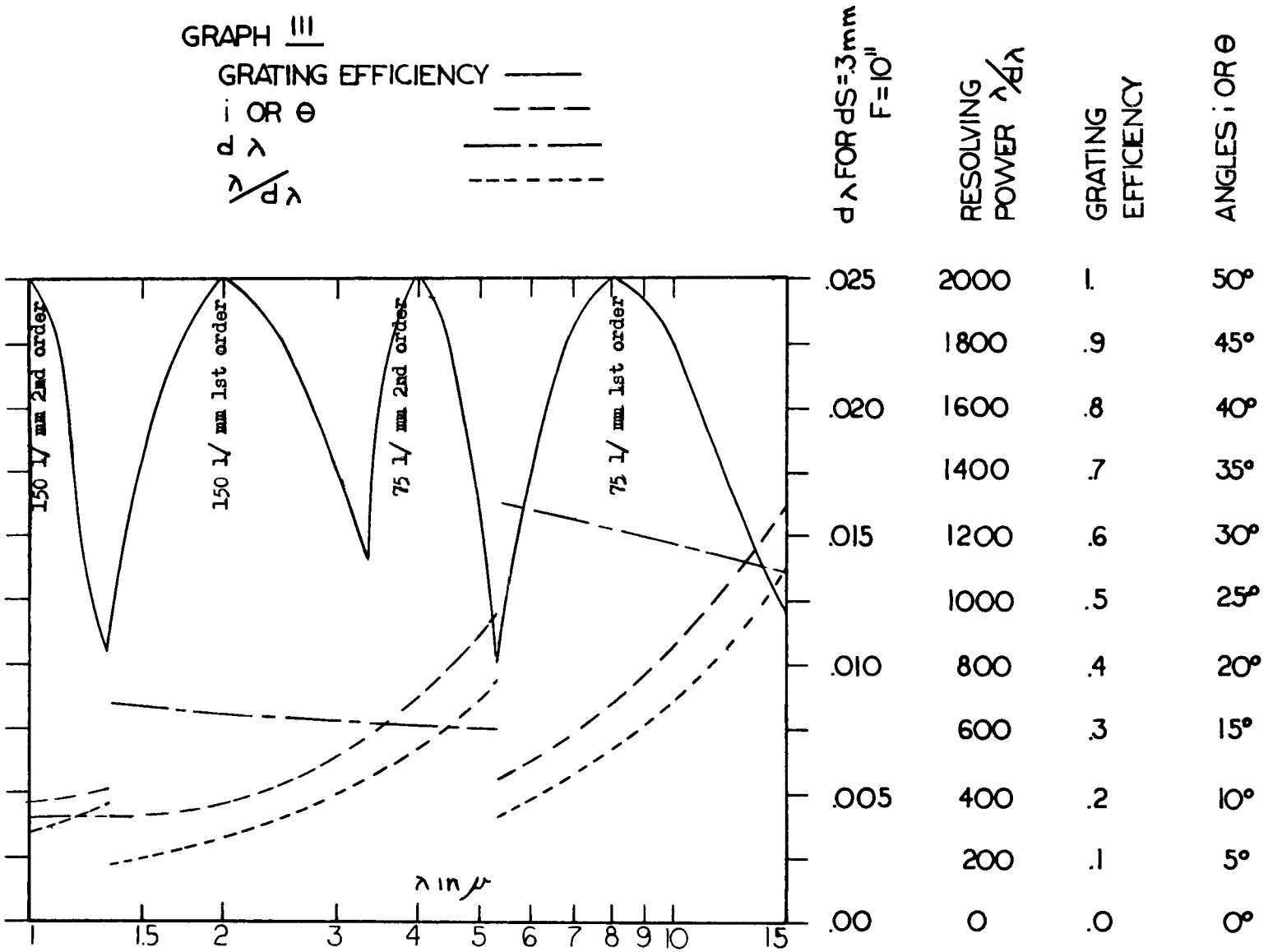
GRAPH III
GRATING EFFICIENCY
i OR θ
d λ
λ/d λ
150 l/ mm 2nd order
150 l/ mm 1st order
75 l/ mm 2nd order
75 l/ mm 1st order
λ in μ
1
1.5
2
3
4
5
6
7
8
9
10
15
d λ FOR dS=3mm F=10"
.025
.020
.015
.010
.005
.00
RESOLVING POWER λ/d λ
2000
1800
1600
1400
1200
1000
800
600
400
200
0
GRATING EFFICIENCY
1.
.9
.8
.7
.6
.5
.4
.3
.2
.1
.0
ANGLES i OR θ
50°
45°
40°
35°
30°
25°
20°
15°
10°
5°
0°

GRAPH IV

GRATING EFFICIENCY ——

i OR θ – – –

d λ —·—

λ/d λ - - - -

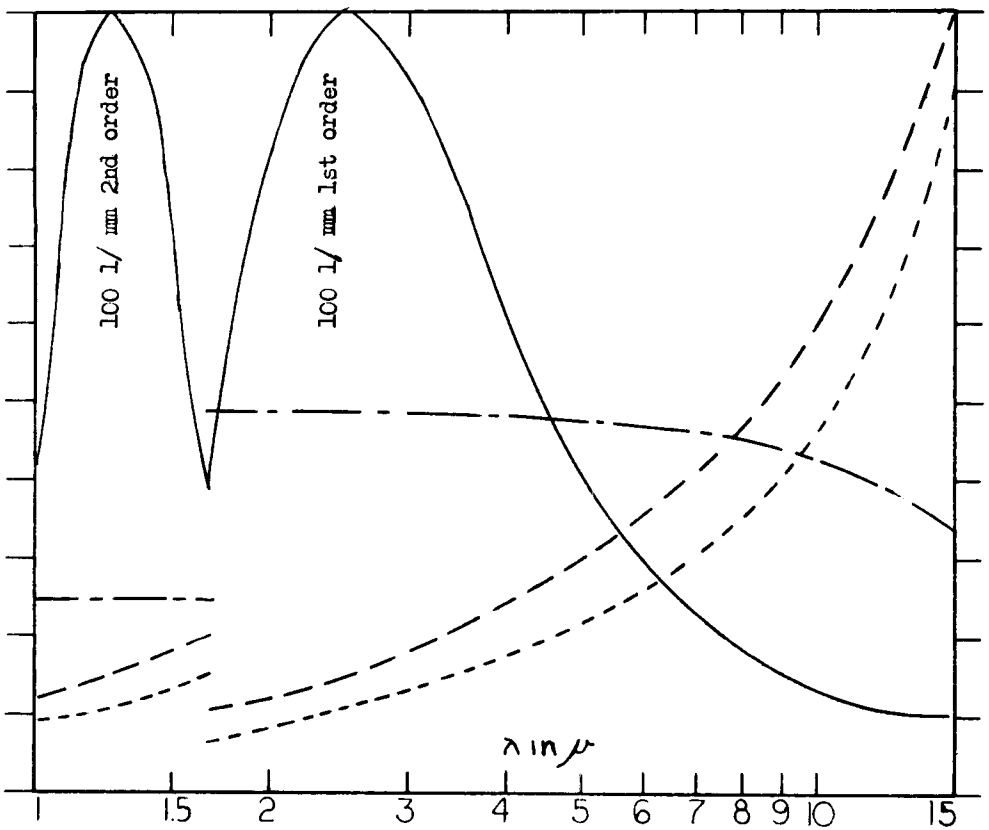

d λ FOR dS=.3mm F=10"	RESOLVING POWER λ/dλ	GRATING EFFICIENCY	ANGLES i OR θ
.025	2000	1.	50°
	1800	.9	45°
.020	1600	.8	40°
	1400	.7	35°
.015	1200	.6	30°
	1000	.5	25°
.010	800	.4	20°
	600	.3	15°
.005	400	.2	10°
	200	.1	5°
.00	0	.0	0°

The resolving powers are low. They range from 260 at 1μ to 1110 at 15μ. The low resolving powers can be doubled by having special gratings made with 600, 250 and 100 1/mm in place of those illustrated.

Graph II shows an arrangement using a 300 1/mm grating in the first order for the wavelength range of 1μ to 5μ, and a 75 1/mm grating is used from 5μ to 15μ. Efficiency between 2.5μ and 5.5μ is very low. This arrangement can be improved some by obtaining special gratings with better blaze wavelengths.

Graph III shows an arrangement using two gratings each used in two orders. A 150 1/mm grating is used in the second order from 1μ to 1.3μ and in the first order from 1.3μ to 3.3μ. A 75 1/mm grating is used in the 2nd order from 3.3μ to 5.4μ and in the 1st order from 5.4μ to 15μ. This arrangement has good energy distribution. It can also be substantially improved by special gratings such as a 200 1/mm and a 100 1/mm in place of the 150 1/mm and 75 1/mm, respectively. Also a better choice of blaze wavelengths is possible.

Graph IV shows the use of a single 100 1/mm grating (special grating) to cover the full wavelength. It is used in the 2nd order from 1μ to 1.7μ and in the 1st order from 1.7μ to 15μ. This single grating will actually cover the large range used this way, but the 10μ to 15μ region is attenuated 10 times. This is the wavelength region where high efficiency is most needed.

Another possible grating arrangement, not shown, is to use a single grating blazed in the 1st order at 8μ for the wavelength range from 5.4μ to 15μ. Its 2nd order would be used from 3.1μ to 5.4μ, the 3rd order from 2.2μ to 3.1μ, the 4th order from 1.7μ to 2.2μ, the 5th order from 1.4μ to 1.7μ, the 6th order from 1.2μ to 1.4μ, the 7th order from 1.05μ to 1.2μ, and finally the 8th order from 1μ to 1.05μ.

This arrangement has a resolving power of only 666 at 1μ for a 100 1/mm grating used in its 8th order.

Beckman proposes that for high photometric reliability and for minimum polarization effects, gratings should be used only in their first order. The subject calibration monochromator is to be used over a wide range of temperatures and in vacuum, its output energy must be a reliable repeatable standard, thus only gratings used in their first orders seem satisfactory.

As shown in Graph I, three different gratings each used in its first order are required to cover the wavelength range of 1μ to 15μ. Beckman proposes either that (1) the three gratings be mounted simultaneously in a mount which automatically switches the proper grating into operating position for each wavelength region, or (2) the gratings may be in individual pre-aligned mounts which allow them to be manually but quickly interchanged. A single linearized wavelength drive cam can serve all gratings.

The dispersion data in the Graphs are for a single monochromator of 10 inch focal length. These values would be doubled by either using a single monochromator of 20 inch focal length or a double monochromator of 10 inch focal length. The values of the Graphs would be 4 times greater for a double monochromator of 20 inch focal length. All of these designs will fit the physical space requirements. Weighing the costs against resolution needs will determine the focal length and number of monochromators to be used. If the requirement of a resolving power of 1000 at .3 mm slit width is more important than cost factors, then the double monochromator with 20 inch focal length is necessary. Also special gratings will be required to obtain an i or θ range for each grating of from approximately 5° or 6° to about 50°.

2.3 Stray Energy

Stray energy is here defined as energy, emitted from the monochromator, made up of wavelengths other than the desired wavelength. For most applications it is required that total stray energy be less than .1% or 1% of the desired wavelength energy, some applications requiring even lower stray energy levels. Stray energy levels lower than .1% for the full wavelength range can be maintained with a prism monochromator in series with the grating monochromator. A system incorporating well designed filters, with an automatic interchange system as a function of wavelength, can hold stray energy levels to below 1.5% without the use of the prism monochromator.

If a prism monochromator is used, only a single grating monochromator is applicable. If filters are used instead of the prism monochromator, a double grating monochromator is usable. Beckman feels that only a careful study of the relative importance of resolution and stray energy will determine whether filters or a prism monochromator should be specified for the calibration monochromator.

2.4 Environment

The temperature range is extreme, and the anticipated temperature variations will create major problems. Some of these major problems are as follows:

1. Expansion and contraction of the grating changes the line spacing and thus alters wavelength calibration. This must be compensated by the way the wavelength cam system is designed to expand and contract.
2. The index of refraction of a prism is altered, thus changing wavelength calibration. This must be compensated by the way the cam shaft system expands and contracts.

3. Filters change their wavelength character, and may have to be tilted angularly to the beam as a function of temperature in order to apply a compensating wavelength shift.

4. If the collimating mirrors and supporting structure have different thermal coefficients of expansion then the monochromator is defocused. Monometalic construction of mirrors and structure is desired if possible.

5. Rotating bearings can either freeze up or become too loose. Care must be taken in their design.

In the final report Beckman will detail the solution for each of these problems.

2.5 Overall Design

The monochromator will be designed for optimal optical performance as determined by race trace studies. The exit slit function will be determined for the full length of the slit and for all incident angles of the gratings and prism if used. An image error map of the aperture will be determined. Such a map is used to evaluate the correctness of focus by a shadow test at the exit slit.

The positions, sizes, and shapes of all elements will be precisely determined by ray trace techniques. Positioning tolerances and component tolerances will be determined for all parts. Any necessary adjustments will be described in detail.